Send Orders for Reprints to reprints@benthamscience.net

Current Medicinal Chemistry, 2020, *27*, 3499-3518

REVIEW ARTICLE

Recent Advances in the Understanding of the Reaction Chemistries of the Heme Catabolizing Enzymes HO and BVR Based on High Resolution Protein Structures

Masakazu Sugishima[1,*], Kei Wada[2] and Keiichi Fukuyama[3,4,*]

[1]*Department of Medical Biochemistry, Kurume University School of Medicine, Kurume, Japan;* [2]*Department of Medical Sciences, University of Miyazaki, Miyazaki, Japan;* [3]*Department of Biological Sciences, Graduate School of Science, Osaka University, Toyonaka, Japan;* [4]*Department of Applied Chemistry, Graduate School of Engineering, Osaka University, Suita, Japan*

ARTICLE HISTORY

Received: August 28, 2018
Revised: November 21, 2018
Accepted: December 11, 2018

DOI:
10.2174/0929867326666181217142715

Abstract: In mammals, catabolism of the heme group is indispensable for life. Heme is first cleaved by the enzyme Heme Oxygenase (HO) to the linear tetrapyrrole Biliverdin IXα (BV), and BV is then converted into bilirubin by Biliverdin Reductase (BVR). HO utilizes three Oxygen molecules (O_2) and seven electrons supplied by NADPH-cytochrome P450 oxidoreductase (CPR) to open the heme ring and BVR reduces BV through the use of NAD(P)H. Structural studies of HOs, including substrate-bound, reaction intermediate-bound, and several specific inhibitor-bound forms, reveal details explaining substrate binding to HO and mechanisms underlying-specific HO reaction progression. Cryo-trapped structures and a time-resolved spectroscopic study examining photolysis of the bond between the distal ligand and heme iron demonstrate how CO, produced during the HO reaction, dissociates from the reaction site with a corresponding conformational change in HO. The complex structure containing HO and CPR provides details of how electrons are transferred to the heme-HO complex. Although the tertiary structure of BVR and its complex with NAD^+ was determined more than 10 years ago, the catalytic residues and the reaction mechanism of BVR remain unknown. A recent crystallographic study examining cyanobacterial BVR in complex with $NADP^+$ and substrate BV provided some clarification regarding these issues. Two BV molecules are bound to BVR in a stacked manner, and one BV may assist in the reductive catalysis of the other BV. In this review, recent advances illustrated by biochemical, spectroscopic, and crystallographic studies detailing the chemistry underlying the molecular mechanism of HO and BVR reactions are presented.

Keywords: X-ray crystallography, Protein structure, Redox complex, Heme metabolism, Enzymatic reaction, Ligand discrimination, Stacked substrate-binding mode.

1. INTRODUCTION

The cofactor heme (iron-protoporphyrin IX) is widely used in various heme proteins; however, as free heme is toxic and produces reactive oxygen species, it should be immediately removed from cells. Heme is catabolized into Biliverdin IXα (BV) and then Bilirubin IXα (BR) in intact organisms. The enzyme involved in heme cleavage to produce BV is Heme Oxygenase (HO) (EC 1.14.14.18), and the enzyme responsible for converting BV into bilirubin is Biliverdin Reductase (BVR) (EC 1.3.1.24). HO was discovered in 1968 by Tenhunen *et al*. and identified as the enzyme that catalyzes oxidative degradation of heme [1, 2]. HO specifically cleaves the α-position of heme to produce a linear tetrapyrrole of BV, Fe^{2+}, and carbon monoxide (CO). HO is essential for recycling iron from heme and is found in both vertebrates and invertebrates. CO, the byproduct of the HO reaction, is a well-known toxic gas, and a small percentage of hemoglobin in erythrocytes binds endogenous CO. Recently, both CO and

*Address correspondence to these authors at the Department of Medical Biochemistry, Kurume University School of Medicine, 67 Asahi-machi, Kurume, Fukuoka 830-0011, Japan;
Tel/Fax: +81-942-31-7544, +81-942-31-4377;
E-mail: sugishima_masakazu@med.kurume-u.ac.jp;
Department of Biological Sciences, Graduate School of Science, Osaka University, Toyonaka, Japan;
E-mail: fukuyama@bio.sci.osaka-u.ac.jp

1875-533X/20 $65.00+.00

NO have been observed to function as important signaling molecules.

CO is involved in inflammation, cell proliferation, and differentiation *via* the NF-*κ*B pathway. This molecule also regulates vasodilation and vasoconstriction *via* cystathionine β-synthase, and circadian rhythms *via* NPAS2 [3-6]. HO is present in higher plants, algae, fungi, and bacteria [7, 8]. Especially, some pathogenic bacteria use mammalian HO homologs to acquire iron from the host heme groups [9].

HO forms a 1:1 complex with the substrate heme and converts it to BV *via* three steps. Specifically, conversion occurs through heme to α-hydroxyheme, then α-hydroxyheme to α-verdoheme, and finally from α-verdoheme to BV (Scheme **1**) [10-12]. CO and ferrous iron are released in the second and third steps, respectively. Mammalian HO requires electrons for these monooxygenase reactions, and these electrons are supplied by NADPH-cytochrome P450 oxidoreductase (CPR) (EC 1.6.2.4).

Mammalian HO enzymes are composed of a soluble catalytic domain and a C-terminal membrane-bound segment. Truncated soluble HO enzymes lacking these C-terminal amino acid residues retained partial activity compared with that of intact HO [13, 14] and were utilized for several biochemical, spectroscopic, and crystallographic studies. Rat and human truncated HOs were over-expressed using *Escherichia coli* [15, 16].

In photosynthetic organisms such as cyanobacteria and plants, BV produced by HO is used to synthesize pigments for light-harvesting complexes of phycobilisomes [17], and light-sensing [18]. Cyanobacterial and plant HOs are soluble proteins that require ferredoxin as an electron donor. BV produced by the HO reaction is further reduced at several specific sites by ferredoxin-dependent bilin reductases resulting in pigments such as phycocyanobilin, phycoerythrobilin, phycourobilin, and phytochromobilin [19-23]. BV, phycocyanobilin, and phytochromobilin function as chromophores for photoreceptors.

BVR catalyzes the reduction of the C10 double bond (α-methene bridge) of BV to yield BR through the use of NAD(P)H as a reducing agent (Scheme **1**). BVR was discovered by J. W. Singleton and L. Laster in 1965 [24]. BR is abundant in blood plasma and is the major antioxidant responsible for protecting cells from H_2O_2 at physiological concentrations [25, 26]. The solubility of BR in bile is increased by glucuronidation catalyzed by glucuronosyl transferase. BR is a source of jaundice, and neonatal jaundice is a common disease in newborns. Jaundice is treated by exposure to blue or white light; as the light converts geometric isomers of BR to increase their solubility [27]. Novel functions of BVR have been reported, and these include a dual-specificity kinase function that regulates the insulin receptor/MAPK pathway and a bZip-type transcription factor function that influences ATF-2/CREB and HO-1

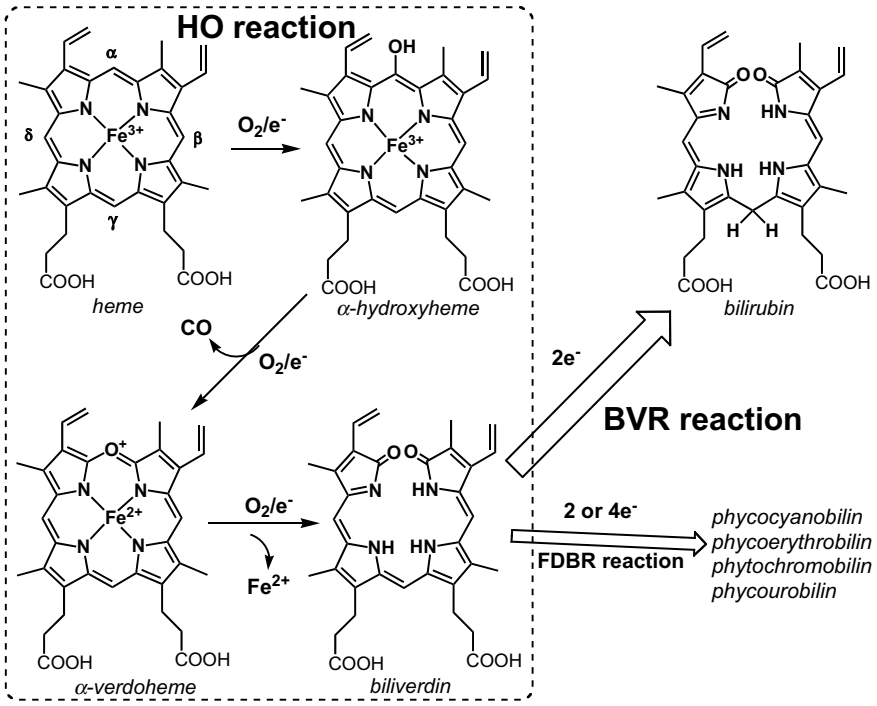

Scheme 1. Heme metabolic pathway.

regulation [28, 29]. The mammalian BVR homolog (BvdR) has been observed in cyanobacteria. When the *bvdR* gene is disrupted in *Synechocystis* sp. PCC 6803, the biosynthesis of phycobiliproteins is disrupted and the biosynthesis of pigments such as phycocyanobilin, which are responsible for photosynthesis, is impaired [30]. Although BR has not been observed in cyanobacterial cells, BvdR is considered to control the biosynthetic pathway of photosynthesis pigments [30].

Mammalian BVRs and cyanobacterial BvdRs are soluble proteins, and crystal structures of rat BVR and its complex with NAD^+ were reported in the early 2000s [31, 32]. Although biochemical studies characterizing the reaction mechanism of these enzymes have been extensively performed, residues involving catalysis or the molecular mechanism to reduce C10 sites using NAD(P)H have not been characterized until recently.

Several reviews discussing HO [12, 33-36] and BVR [37-39] have been published in the last few decades. This review describes recent studies detailing the properties, structures, and molecular mechanisms of heme catabolizing HO and BVR enzymes.

2. PROPERTIES OF HO

Mammalian HOs are proteins weighing approximately 33 kDa, and the C-terminal segment is anchored to the microsomal membrane. Truncated soluble HO forms a monomer, but oligomerization of HO is thought to occur in intact HO-1 [40]. There are two isoforms of this protein, HO-1 and HO-2. HO-1 is highly expressed in the spleen and liver and is responsible for degradation of heme-derived mainly from senescent erythrocytes. HO-2 is fully refractory to the inducers for HO-1, and it is constitutively expressed in the brain and testis [41]. HOs of cyanobacteria and plants are soluble proteins and exist as several isoforms.

HO binds to heme at a specific position to form the heme-HO complex and then activates molecular Oxygen (O_2) using the substrate heme [42]. The heme complex of HO exhibits spectroscopic properties similar to those of other heme proteins such as myoglobin and hemoglobin [43, 44]. The ferric heme-HO complex exists in a six-coordinate high spin state at neutral pH, and it converts into a low spin state at basic pH based on Raman and EPR spectroscopy analysis [44]. The conserved His residue located near the N-terminus is thought to act as the ligand for the heme iron.

One characteristic of heme-HO is that it exhibits an affinity for CO that is almost equal to that for O_2 in heme-HO. The parameters describing O_2 and CO binding to heme-HO complexes are given in (Table **1)** [45]. It is well established that the affinity of other heme proteins such as myoglobin and hemoglobin for CO is much higher than that for O_2.

2.1. Activity of HO, Assignment of Catalytic Residues, and Structural Details of Mammalian HOs Complexed with Heme

Activation of O_2 is the key process in HO reaction. Region-specific oxidation of heme is thought to involve the carboxylate amino acid side chain of HO [46]. Initially, the residues located at the distal side of the heme iron were investigated by biochemical and mutational studies [47, 48]. When the conserved aspartic acid residue at position 140 was replaced with residues such as histidine, asparagine, or alanine, HO activity was severely affected, indicating involvement in the activation of O_2 [47, 48].

Human and rat HO-1s that had undergone removal of the C-terminal membrane anchor to increase solubil-

Table 1. Association constants for O_2 and CO binding to heme HO complexes, human myoglobin, and leghemoglobin (Data are taken from Migita *et al.* [45]). Association constants of CO binding to HO have two parameters because CO binding to HO is biphasic.

Protein	O_2 binding (μM^{-1})	CO binding (μM^{-1})	Ratio (K_{co}/K_{o2})
HO-1	28	150	5.4
		34	1.2
HO-2	77	420	5.5
		89	1.2
Myoglobin	0.86	35	41
Leghemoglobin	23	2200	95

ity were crystallized in complex with heme [49, 50] and resolved by X-ray crystallographic analyses [51, 52].

HO is an α-helical protein (Fig. **1**). The heme group is surrounded by A-, B-, and F-helices, and the heme iron is coordinated by the His residue (His25 in both rat HO and human HO) in the A-helix. The F-helix is kinked on the distal side of heme. Interestingly, there is no side chain on the distal side of heme; the closest residue to the heme iron is glycine. Crystal structure analysis revealed that a water molecule or OH^- is coordinated to the heme iron in the ferric heme bound state. The orientation of the heme is maintained by the electrostatic interactions between basic residues of HO and two heme propionate groups. Close examination of the electron density map revealed that a small fraction of the heme was bound to HO in an inverted manner around the axis connecting the α and γ positions, which is consistent with the NMR analysis results [53].

There was no amino-acid residue, such as histidine or aspartic acid, located at the distal side of the heme group. Instead, a conserved hydrogen-bond network was present that connects the O_2 substrate with Asp140 and Arg136 on the distal side through the use of water molecules (Fig. **1B**). The essential catalytic residue Asp140 was located relatively far from the heme distal side. Participation of the hydrogen bond network in the active site of HO was studied by NMR spectroscopy [54]. The catalytic mechanism of HO (*i.e.* conversion of heme to α-hydroxyheme) was also studied by EPR and ENDOR spectroscopy, and Asp140 mutants were prepared to test if a water molecule stabilizes the hydroperoxy species [55].

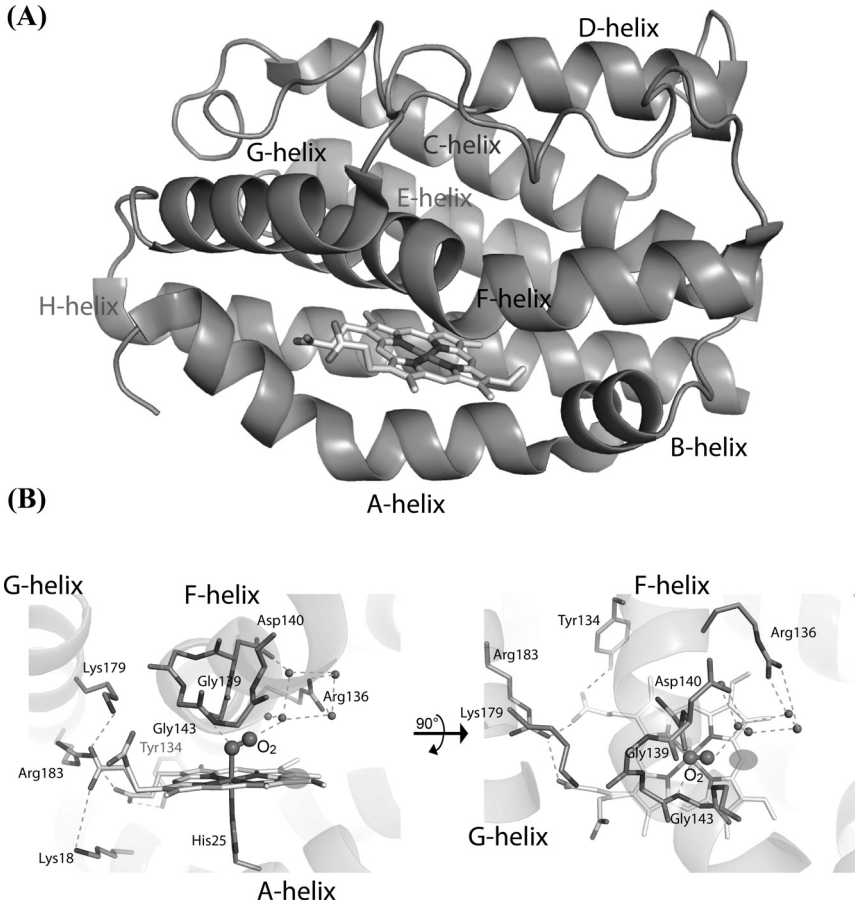

Fig. (1). Crystal structure of rat HO-1. (**A**) Overall folding of rat HO-1 in complex with heme. Eight helices were denoted as A to H. Heme is located between A- and F-helices. (**B**) Close-up view of heme environments of the O_2 bound heme-rat HO-1 complex viewed from the distal side. At the proximal side, the heme iron is coordinated by the histidine Nε atom (His25 in the case of rat HO-1). At the distal side, O_2 is coordinated. F-helix is kinked on the distal side as the surrounding of O_2. O_2 is directed to the α-meso site of heme (shaded circle). Two propionate groups of heme are anchored by several salt bridges to fix the orientation of heme. Asp140, the catalytic residue, is connected to O_2 *via* several water molecules.

The structure of another mutant human heme-HO-2 complex, where C-terminal residues including the Heme Regulatory Motif (HRM) [56] and the membrane anchor were truncated, was also determined. Overall, the heme-binding site structure in HO-2 resembled that of HO-1 [57].

2.2. Structural Changes in HO Upon Heme Binding

In the crystal structure of rat apoHO-1 a large conformational change occurred at the heme-binding site upon heme binding [58]. In rat apoHO-1, the N-terminal A-helix was not clearly visible in the electron density map, and the B-helix was shifted to shrink the heme pocket relative to that of rat heme-HO-1. The kinked region of the F-helix exhibited altered conformation and appeared flexible. These changes indicate that when the heme binds to HO, the heme is fixed by salt bridges formed between the propionate groups and Lys18, Lys179, and Arg183 and by hydrogen bond formation between the propionate group and Tyr134. The Nε atom of His25 coordinated with the heme iron at the proximal side, and a hydrogen bond network was formed at the distal side (Fig. **1B**).

Crystal structures of human apoHO-1 and bacterial apoHO were determined at a higher resolution than those of rat apoHO-1 [59, 60]. A-helices are visible and some conformational changes observed in these structures were not seen rat apoHO-1. Similar to what was observed in rat apoHO-1, the hydrogen bond network at the distal side was absent in apo-HO.

The conformational dynamics of rat HO-1 were determined using NMR as a means to elucidate the mechanism by which HO-1 recognizes heme (Fig. **2**) [61]. NMR relaxation experiments showed that, as observed in the crystal structures, rat apoHO-1 A-, B-, and F-helices fluctuate, and in concert with a surface-exposed loop (CD-loop) and the CD-loop transiently form a partially unfolded structure. The fluctuating CD-loop is located more than 17 Å from the heme-binding site, and the function of this loop is unknown. While attempting to elucidate the function of this loop, we found interesting mutations that altered activity but caused little change in conformation. The Phe79Ala mutation in the CD loop is involved in regulating the conformational change for heme binding by promoting conformational fluctuations. Further, the CD-loop is close to the interaction site for CPR in the CPR-HO complex as shown in below (Fig. **6A**). Thus, the binding of heme to HO-1 may affect the affinity of CPR for HO-1 through the control of fluctuations in the heme-binding site and the CD loop.

2.3. Structures of Molecular Oxygen (O_2)-, Azide-, and Nitric Oxide-Bound Heme-HO

The crystal structure of the O_2-bound form of rat heme-HO-1 was determined at a 1.8 Å resolution. O_2 was bound to the heme iron and the angle of Fe-O-O was 118° [62], which is consistent with a previous resonance Raman spectroscopic study [63]. The hydrogen bond network of these HOs was essentially the same as that of the native heme-HO complex (Fig. **1B**) and formed a hydrogen bond with the distal oxygen atom of O_2. The amide group of Gly143 located in the F-helix formed a hydrogen bond with the proximal oxygen atom of O_2. These hydrogen bonds increased O_2 affinity for the heme-HO complex. Similar binding of O_2 to the heme-HO complex derived from *Corynebacterium diphtheriae*, heme-HmuO, was observed in a crystallographic study [64]. Substrate O_2 was similarly bound to the heme iron; and the angle of Fe-O-O was 101-114°. The amino group of the Gly residue on the distal side was also directed toward O_2. O_2 analogs (az-

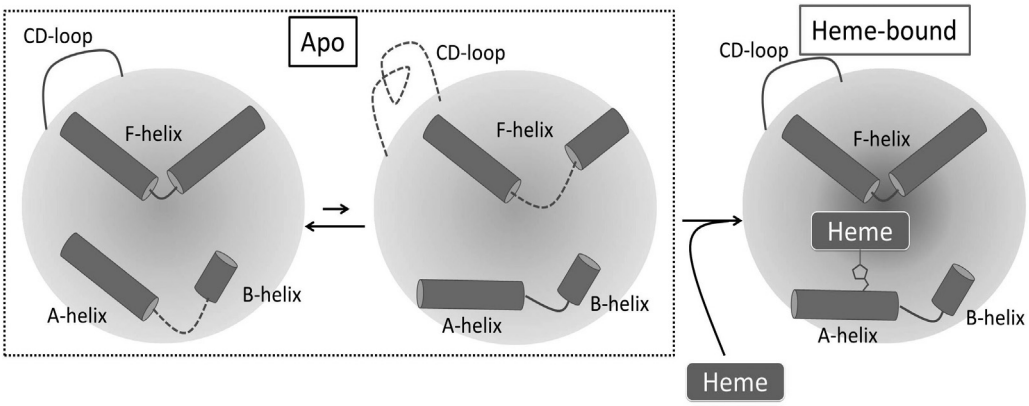

Fig. (2). Conformational dynamics of apo HO-1. In apo HO-1, A- and B-helices fluctuate for heme binding, and the F-helix and CD-loop are partially unfolded in the minor state as shown by dotted lines.

ide and nitric oxide) also bound similarly to the heme iron of rat heme-HO [65, 66]. Thus, the O_2 and O_2-like ligand-binding mode is named the bent mode.

All ligands were directed toward the α-position of heme (Fig. **1B**). As the F-helix is kinked at Ser142 to allow envelopment of the distal ligand, distal ligands cannot achieve any position other than the α-position. As a result, HO specifically cleaves the α-position of heme. Although a small fraction of heme was bound to HO in an inverted way connecting the α and γ positions, the cleavage site of the α-position was not affected.

2.4. Conformational Changes Resulting from CO or Cyanide Binding to Heme-HO

Unlike with substrate O_2 or the inhibitors azide and nitric oxide, the angle of Fe-C-O was 158° in the CO bound heme-rat HO-1 complex, which is nearly linear (Fig. **3**). This binding mode is described as the tilt mode. Cyanide bound similarly to the heme iron [65].

Notably, upon CO or cyanide binding to the heme iron, the F-helix shifts by about 1.0 Å to avoid steric hindrance between the ligand and the F-helix (Fig. **3**). Consequently, the proximal histidine shifts along with bound heme result in breakage of the hydrogen bond between heme propionate and Lys179. Additionally, when the Fe-CO bond was photolyzed in the CO bound heme-rat HO-1 crystal, reverse conformational changes of the distal F-helix and the heme iron were observed (Fig. **4**) [62]. Such dynamic structural changes in the heme-heme HO-1 complex following CO dissociation were also observed by time-resolved resonance Raman spectroscopy [67]. Temporal changes in resonance Raman bands at the Fe-His stretch and the heme propionate bends were observed at the sub-nanosecond and microsecond time regime, respectively. These changes suggest structural rearrangements in the Fe-His linkage and the salt bridges of heme propionates following CO dissociation. The Fe-His stretching mode exhibited an upshift up to 30 μs after dissociation. This is the first example of an upshift in CO-dissociation-induced stretching of the Fe-His linkage in heme proteins.

2.5. Discrimination of O_2 and CO by HO

HO is unique in that it is able to utilize O_2 molecules in the presence of CO. Biochemical studies have shown that O_2 dissociation rates are remarkably slow, indicating that favorable interactions occur between bound O_2 and protein residues in the heme pocket (Table **1**) [45]. Free heme binds CO with a significantly greater affinity compared to that for O_2, and this affinity difference can be as high as 10^4 fold. It is well known that O_2 binds the heme iron with a bent mode, while CO binds with a tilt mode. Such stereochemical constraints may explain why the iron atom of heme-HO/α-hydroxyheme-HO/verdoheme-HO poorly binds to CO. The bent mode ligand of O_2 interacts at the dis-

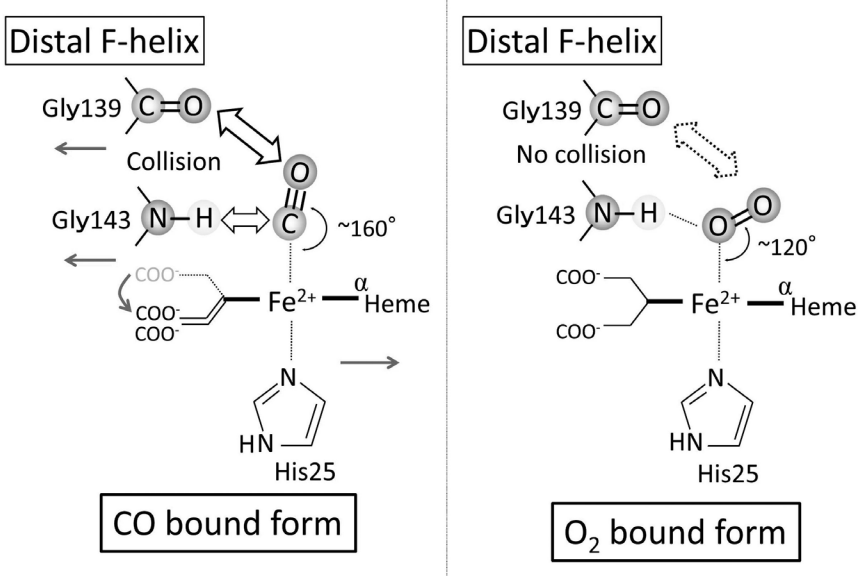

Fig. (3). Two mechanisms of ligand bindings by O_2 and CO. O_2 is bound to the heme iron with a bent mode; the angles of Fe-O-O are approximately 120°. When O_2 binds to heme-HO, no conformation change occurs, as there is no collision between O_2 and Gly139. CO is bound to the heme iron with a tilt mode, and the angles of Fe-C-O are approximately 160°. When CO binds to heme-HO, a subtle conformation change is induced allowing escape from the steric hindrance between CO and the carbonyl group of Gly139.

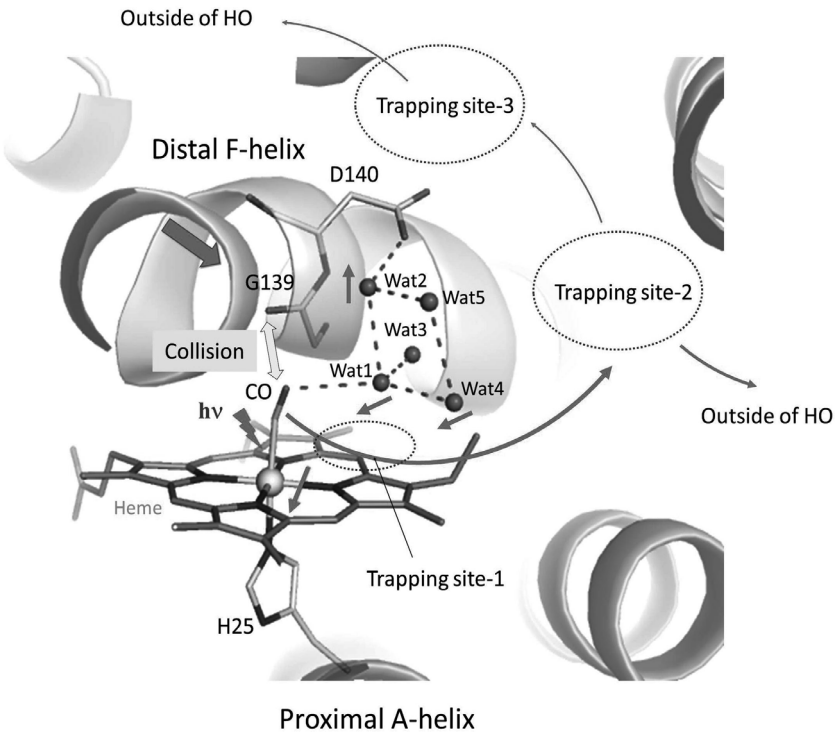

Fig. (4). Conformation change after CO photolysis in the CO-heme-rat HO-1 crystal and the pathway of photolyzed CO escape from the heme pocket.

tal side and causes no steric hindrance at the F-helix, however, CO binding does result in steric hindrance at the F-helix. Additionally, the NH group of Gly143 (rat HO-1) orients the bound O_2 and the proximal oxygen atom of O_2 acts as the acceptor of the NH···O hydrogen bond, while a hydrogen bond between CO and Gly143 is unlikely (Fig. **3**) [65]. These observations provide an explanation for the increased affinity for HO to O_2 as opposed to CO. A similar O_2/CO discrimination mechanism was reported for heme-HOs from *Neisseria meningitides* and *Pseudomonas aeruginosa* [68].

2.6. Conduits for Gaseous Molecules to Escape from the Heme Pocket of HO

While CO is generated from the carbon atom at the α-position of heme during the HO reaction, the location of CO transiently trapped within HO remains unclear. CO is generated in the second step of the HO reaction, and O_2 is necessary for progression to the third step (Scheme **1**). It is established that CO binds more tightly to the heme iron than does O_2, and given this it remains unclear as to how HO can proceed to the third reaction step, which requires O_2 when CO is present.

Rather than using enzymatically evolved CO, we instead used red laser illumination to release CO from the CO-heme-HO complex to examine the CO trapping site under liquid helium temperatures (ca. 35 K) [69]. Photolyzed CO was sequestered within a cavity surrounded by hydrophobic phenylalanine and methionine residues in proximity to the heme group (Trapping site-2, Fig. **4**). Xenon, which is normally bound at the photolyzed CO trapped site, was also bound within the hydrophobic cavity. These residues are conserved in mammalian, cyanobacterial, plant, and bacterial HOs. At 160 K, an additional trapping site was observed at the rear of the distal heme pocket (Fig. **4**, Trapping site-3) [62].

2.7. Conversion of Heme to α-Verdoheme *Via* α-Hydroxyheme by HO

The α-methene bridge of heme is oxidatively hydroxylated by HO to produce α-hydroxyheme, a compound in which the O_2 molecule is activated on the heme iron and the α-position of heme is hydroxylated (Scheme **1**). HO subsequently uses O_2 to convert α-hydroxyheme into α-verdoheme the concomitant release of CO. This step has been studied biochemically and monitored by EPR and absorption optical spectroscopies to show that the reaction proceeds in the presence of O_2, but not reducing equivalents [70, 71]. Characteristic bands of verdoheme and CO-verdoheme species at 690 nm and 638 nm were observed after the addition of 1.3 eq. of O_2 to the ferric α-hydroxyheme-rat HO-1 complex [72].

HO subsequently uses O_2 to convert α-verdoheme into ferric BV-iron chelate. This step and the first step of the HO reaction can be bypassed by using H_2O_2. Asp140 is critical for both steps [73].

The crystal structure of ferrous α-verdoheme complexed with rat HO-1 was determined, and this complex was prepared by reconstitution with chemically synthesized α-verdoheme. The overall structure of the complex was similar to that of the heme-HO complex [74]. Water or OH^- was coordinated to the α-verdoheme iron as a distal ligand. Similar to what was observed in the heme-HO complex, a hydrogen bond network consisting of water molecules and several amino acid residues at the distal side of α-verdoheme was conserved. This network may act as a proton donor to form an activated oxygen intermediate, likely a ferric hydroperoxide species, in the degradation of α-verdoheme to ferric BV-iron chelate. This event is similar to what occurs during the first oxygenation step.

The crystal structures of ferrous verdoheme-bound and NO-verdoheme-bound human HO-1 have been reported [75]. Due to limited resolution, a detailed description of heme ligand geometry is uncertain.

2.8. Structure of the Ferric BV-Iron Chelate Bound HO

When the third step of HO reaction is completed, the heme cleavage product, ferric BV-iron chelate, is produced, and the Fe^{2+} ion and BV are released from HO. The crystal structure of the ferric BV-iron chelate-bound rat HO-1 was determined, and the tetrapyrrole portion of the ferric BV-iron chelate exhibited a distorted U-shaped conformation (ZZZ, sss configuration) (Fig. **5**) [76]. One propionate group exposed to the surface was not detected in the electron density map. The distances from the iron atom to the five nitrogen atoms, including Nε atom of His25, increased relative to those observed in the heme-HO-complex. The hydrogen bond network including Asp140 was retained. When this structure was compared with the verdoheme-HO structure, the conformation of the heme distal side was significantly altered. The hydrogen-bonding scheme of the kinked site of the F-helix was altered from a π-helical conformation to an α helical conformation, and the hydrogen bond partner of the carbonyl group of Gly139 was altered from the amide group of Gly144 to that of Gly143. The subtle change resulted in an altered orientation of the F-helix and the heme pocket became wider. Consequently, the Fe^{3+} atom and BV can be released from HO, when the Fe^{3+} atom is reduced.

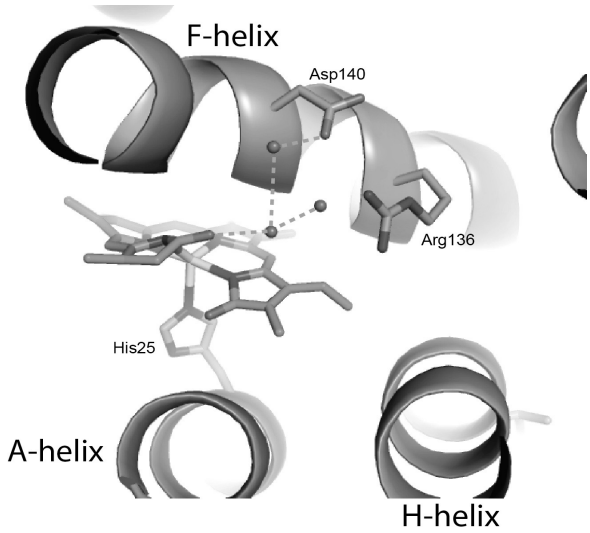

Fig. (5). Close-up view of the BV-iron chelate bound HO structure. BV-iron chelate and the distal hydrogen-bond network are shown as stick models.

2.9. Interaction Between the Heme-HO Complex and CPR

The electrons required for HO catalysis in mammals are provided by CPR, a 78 kDa membrane-bound microsomal flavoprotein, containing one molecule each of FAD and FMN. The structure of rat CPR was reported to contain three domains, including the FMN-binding domain, the connecting domain, and the FAD-binding domains spanning the N- to C-termini. The first reported rat CPR structure existed as a closed form in which FAD and FMN exist in proximity to one another. Thus, the closed form is appropriate for intra-electron transfer from NADPH to FMN *via* FAD [77]. The closed form is, however, inappropriate for inter-electron transfer to the partner enzyme, as FMN is not exposed to the surface. Small angle X-ray scattering, ion mobility mass spectroscopic, and fluorescence energy transfer studies demonstrated that CPR could change its conformation from a closed to an open form [78-81]. These studies suggest that large conformational changes in CPR occur during charge transfer from CPR to HO.

As the heme-rat HO-1 complex formed a stable complex where the open form stabilized the rat CPR mutant (ΔTGEE) [82], we crystallized the ΔTGEE-heme-rat HO-1 complex and determined its crystal structure at a 4.3 Å resolution (Fig. **6A**) [83]. Interestingly, both the FMN binding domain and the FAD binding domain were involved in the interaction with

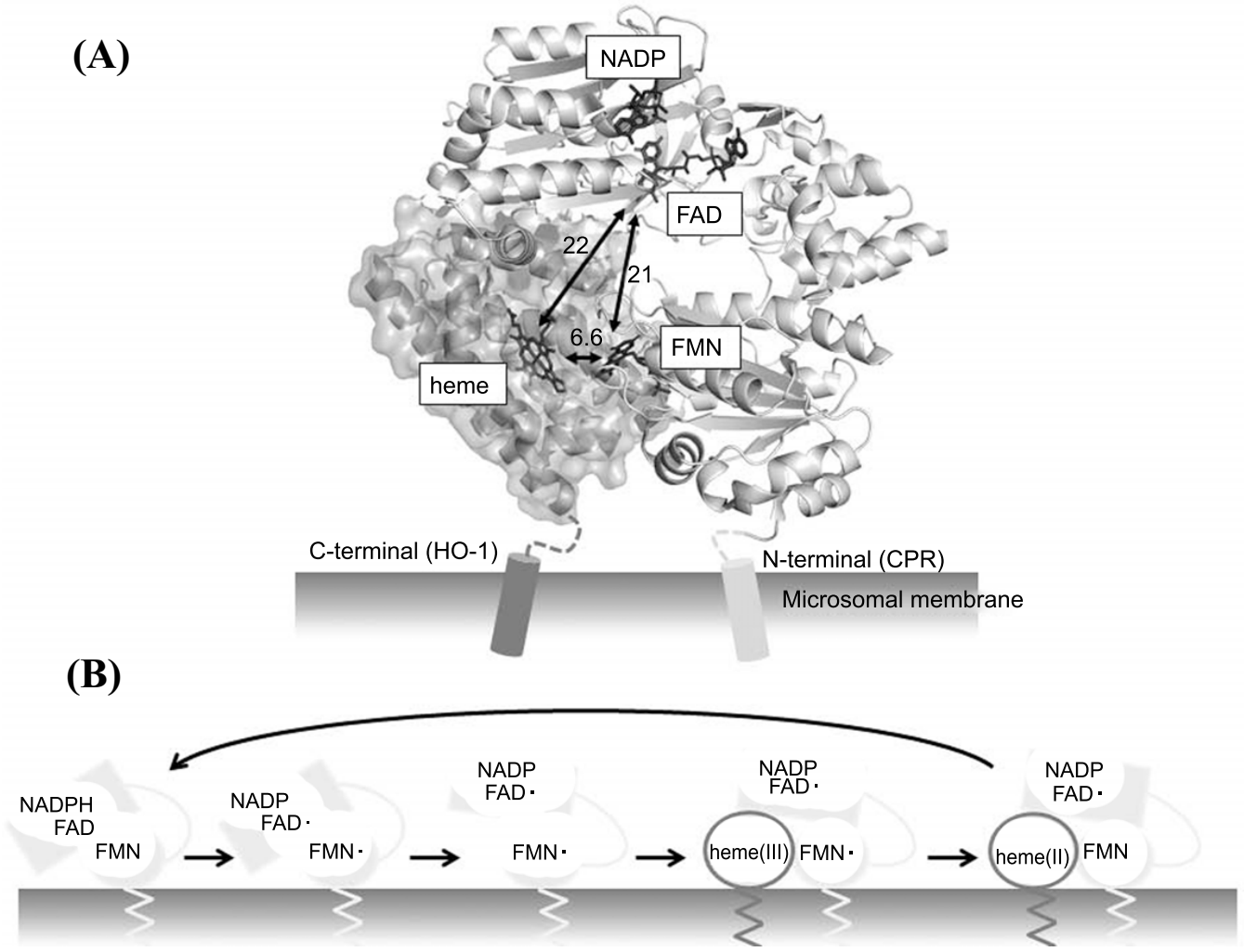

Fig. (6). Electron transfer from CPR to heme with large conformation changes in CPR. (**A**) The structure of the complex of the open form of CPR and heme-HO-1. HO-1 is shown as molecular surface with a ribbon diagram. The heme bound to HO-1 is close to the edge of the isoalloxadine ring of FMN bound to CPR. In the open form of CPR, the distance between FAD and FMN is too large for smooth electron transfer. (**B**) The proposed scheme of electron transfer from CPR to HO. One electron reduced flavin cofactors are shown as FAD· and FMN·. Ferric and ferrous heme are displayed as heme (III) and heme (II), respectively.

heme-HO. Site-specific mutation and biochemical and physicochemical studies showed that Arg185 and Lys149 residues located in the F-helix of rat-HO-1 are involved in both HO activity and its association with CPR [84, 85]. These residues are located at the interface between HO and CPR. The CD loop of HO-1 exists adjacent to the FAD-binding domain of CPR. As indicated above, the dynamics of the CD loop are regulated by the binding of heme to HO-1 (Fig. **2**). As apoHO-1 did not form a stable complex with ΔTGEE [83], the distal regulation of the conformation of the CD-loop by heme binding may control the interaction of HO-1 with CPR. The structure of the CPR and heme-HO complex revealed the mechanisms by which electrons are transferred from CPR to the heme-HO. Initially, transfer occurs from NADPH to FAD, and then from FAD to FMN in the closed form. The CPR conformation may then change from the closed to the open form, and a complex is formed between CPR and heme-HO. Within the CPR-heme-HO complex, FMN is located in close proximity to heme, and thus, an electron can readily transfer from FMN to heme resulting in the reduction of the heme-iron. Finally, CPR conformation changes from an open to closed form, and dissociation from the heme-HO occurs (Fig. **6B**).

The HO reaction requires seven electrons, and thus seven cycles of CPR conformation changes are required for a single turnover reaction catalyzed by HO. Despite this, a biochemical study has indicated that FMN-depleted CPR can transfer electrons to the

verdoheme-HO-1 complex to produce the BV-iron chelate [86]. In the present CPR-heme-HO complex, FAD distant from the heme iron, resulting in difficulties in electron transfer from FAD to the verdoheme iron if the binding mode of CPR to the verdoheme-HO-1 complex is similar to that of the heme-HO-1 complex. Thus, another unknown binding mode of CPR may be utilized for the conversion of verdoheme to BV-iron chelate.

2.10. Cyanobacterial HO in Complex with Heme

Cyanobacteria and plants also express HOs, and electrons are supplied to HO by ferredoxin. Ferredoxin is a small acidic protein that contains one [2Fe-2S] cluster at its molecular surface [87]. Cyanobacterium of *Synechocystis* sp. PCC 6803 express two isoforms of HO-1 and HO-2 (Syn HO-1 and HO-2). In contrast to the expression pattern of mammalian HO-1 and HO-2, Syn HO-1 is constitutively expressed and essential for aerobic growth, while Syn HO-2 expression is induced under micro-oxic conditions [88]. Cyanobacterial and plant HOs are used to convert heme to BV, which are utilized to synthesize various pigments involved in photosynthesis and light sensing [19, 22, 89, 90]. The crystal structures of the heme complex of Syn HO-1 and Syn HO-2 were determined, and both possess folding similar to the catalytic domain of mammalian HOs [91, 92]. Unlike other soluble or solubilized HOs, Syn HO-2 formed a dimer with unclear, physiological significance. Although the crystal structure of the ferredoxin-Syn HO-1 complex is unknown, the positively charged surface of Syn HO-1 is narrower than that of rat HO-1. The electrostatic characteristics of Syn HO-1 appear to support interaction with ferredoxin.

2.11. Pathogenic Bacterial HO in Complex with Heme

Although many bacteria harbor heme degradation enzymes that are not related to mammalian HO, some pathogenic bacteria express a mammalian HO homolog that allows for the acquisition of iron atoms from the heme of host cells. The crystal structures of heme complexed with HOs from *Corynebacterium diphtheria*, *Neisseria meningitides*, and *Pseudomonas aeruginosa* have been determined [93-95]. These HOs are shorter than mammalian HOs and lack the C-terminal membrane anchor region. Although a few helices are replaced by flexible loops in bacterial HOs, the overall folding of bacterial, mammalian, and cyanobacterial HOs is similar. HO derived from *Pseudomonas aeruginosa* exhibits altered region specificity; biliverdin IXδ is the major product of this HO. The heme-bound to *Pseudomonas aeruginosa* HO is rotated by approximately 100° compared with heme bound to other HOs.

The imidazole group of the histidine residue coordinates with the heme iron at the proximal side. There is also a hydrogen network located at the distal side of the heme group, and this network connects the iron-bound water ligand of the water molecules. This enables proton transfer from the solvent to the catalytic site, and oxygen activation occurs, in a manner similar to that of mammalian HO. Proximal and distal helices shift closer to the heme plane in the ferrous heme complex than they do in the ferric heme complex.

The crystal structures of the apo form, O_2-bound form, verdoheme-bound form, and biliverdin-bound form were also reported using HO from *Corynebacterium diphtheria* [60, 64, 96, 97]. These structures are similar to those of mammalian HOs.

2.12. Compounds that Inhibit HO Activity

Several types of HO inhibitors, including metalloporphyrin inhibitors, have been characterized [98]. Among these HO inhibitors, azalanstat analogues (imidazole-dioxolane compounds) were synthesized as inhibitors of mammalian HOs (Scheme **2**).

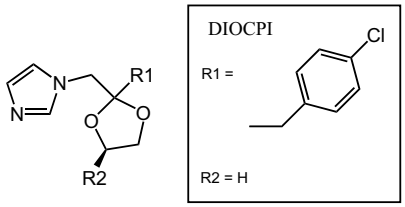

Scheme 2. Chemical structure of the imidazole-dioxolane compound.

The characteristic feature of such inhibitors is selectivity between the inducible HO-1 and constitutive HO-2 enzymes [99-101]. To determine the binding mode of these compounds to HO and the underlying inhibitory mechanism, the crystal structure of the complex between one representative compound, 2-[2-(4-chlorophenyl)ethyl]-2-[(1*H*-imidazole-1-yl)methyl]-1,3-dioxolane (DIOCPI) and rat HO-1 was determined [102].

DIOCPI was bound to the heme iron at the distal side of the heme plane. The nitrogen atom of the imidazole ring coordinated with the heme iron at the substrate O_2 binding site.

The bulky inhibitor molecule occupied the narrow distal pocket, resulting in an open conformation of the distal F-helix and replacement of the distal hydrogen

bond network. The propionate group of heme exhibited conformational changes similar to those induced by CO. The 4-chlorophenyl group of DIOCPI occupied the hydrophobic cavity composed of the side chains of phenylalanine and methionine residues where CO is transiently trapped [69]. DIOCPI occupies the distal site of the heme iron, and thus appears to inhibit the conversion of ferrous heme-HO to O_2-heme-HO in a competitive manner. Our biochemical study, however, demonstrated that DIOCPI severely inhibits the conversion of verdoheme to BV-iron chelate [102].

A variety of compounds have been synthesized to selectively inhibit HO-1 and HO-2, and examination of the binding modes of related imidazole-dioxolane compounds to human HO-1 revealed that all of these compounds bound to HO-1 in a similar manner [103-107]. Although inhibitors exhibiting high selectivity were examined extensively, the structural mechanisms underlying the selectivity of these compounds for HO-1 and HO-2 remain uncertain as the structures of the heme pocket and the hydrophobic cavity of HO-1 are very similar to those of HO-2 [57].

Alternative compounds were reported to bind at the distal side of heme, and these compounds inhibit HO activity by disrupting the hydrogen bond network [108]. D,L-dithiothreitol (DTT) and dithioerythritol (DTE) bind mammalian HO with high affinity. DTE shows high selectivity for HO-1 rather than HO-2. The crystal structures of DTT- and DTE-bound rat heme-HO-1 and heme-HmuO were determined. DTT binds to the heme iron at the terminal thiol group, and two hydroxyl groups interact with environmental amino acids. In both DTT-heme-HO-1 and DTE-heme-HmuO complexes, DTT and/or DTE occupy the heme distal side, and the hydrogen bond network essential for the HO reaction is absent.

3. PROPERTIES OF BVR

In mammals, BV generated by HO is further converted to BR by BVR (Scheme **3**) [24]. BVRs were isolated and purified from the rat liver, pig spleen, and human liver [109-111]. BVR has been reported to exist as two isomers, BVR-A and BVR-B. BVR-A is the major form of BVR in the adult human liver and catalyzes the reduction of BV(IXα), a heme-cleavage product at the α-position, into BR(IXα). BV(IXβ), another heme-cleavage product at the β-position, is reduced by BVR-B to form BR(IXβ). In adult humans, the ratio of BV isomers is 95-97% IXα and 3-5% IXβ.

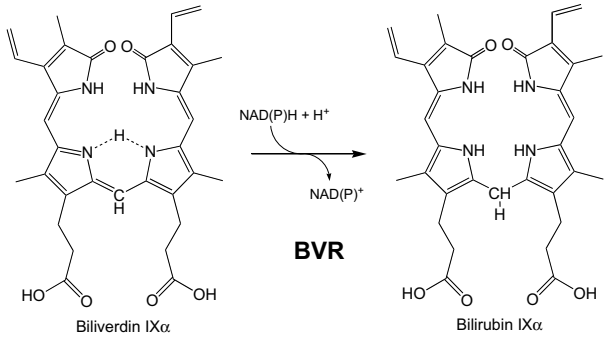

Scheme 3. BV reduction by BVR.

This ratio does not change significantly under various physiological and pathological conditions [112]. In this review, we focus on BVR-A (BVR indicates BVR-A, unless otherwise stated), and we describe recent updates concerning the biochemical and structural features of BVR.

BVR catalyzes reduction of the double bond at the C10 position of BV to generate BR. NADH or NADPH supplies a hydride (H^-) for the reaction. A recent study indicated that certain BVRs from *Actinobacteria* utilize the F_{420} cofactor, a deazaflavin cofactor, instead of NAD(P)H [113]. BVR possesses two distinct pH optima depending on if NADH or NADPH is used during the enzymatic reaction. NADH is preferentially used at pH 6-7, whereas NADPH is used at approximate pH 8.5 [110]. The enzymatic activity with NADH as a cofactor is enhanced by inorganic phosphate, likely by mimicking the 2'-phosphate of NADPH in stabilizing the interaction between NADP and BVR [114]. In addition, some cyanobacteria, including the model organism *Synechocysitis* sp. PCC 6803, express a mammalian BVR homolog, BvdR [30]. BvdR possesses an acidic pH optimum for enzymatic activity to convert BV to BR, and NADPH is preferentially used at all pH values [30].

3.1. Crystal Structures of BVR

Rat BVR was crystalized and its crystal structure was determined in the early 2000s [31, 115]. BVR consists of two domains, the N-terminal dinucleotide-binding domain and the C-terminal domain (Fig. **7**). The N-terminal dinucleotide binding domain consists of an α/β dinucleotide-binding motif, which is a typical Rossmann fold in which a parallel β-sheet is surrounded by six α-helices. The most striking feature of the C-terminal domain is a large, flat, six-stranded β-sheet. One face of this sheet presents predominantly polar and charged residues to the solvent, resulting in

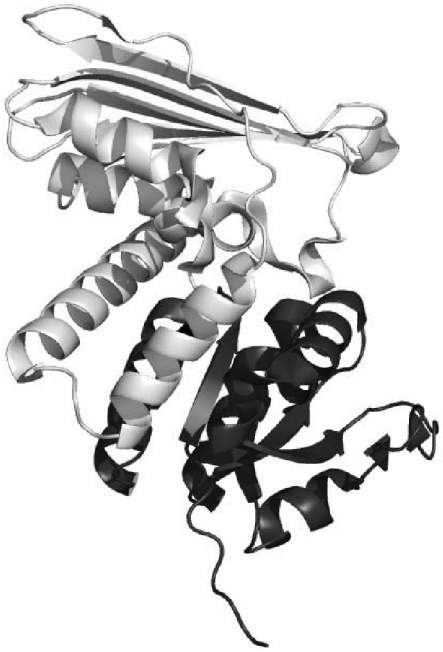

Fig. (7). The structure of rat BVR. BVR possesses an N-terminal dinucleotide binding domain (black) and a C-terminal domain (gray). The NAD^+ at the N-terminal domain is bound to a typical Rossmann-fold motif. (*A higher resolution / colour version of this figure is available in the electronic copy of the article*).

the formation of a planar surface at one end of the molecule. The crystal structure of rat BVR in complex with NAD^+ was also determined, and NAD^+ was bound to the crevice between the N- and C-terminal domains [32]. In rat BVR, the residues surrounding the hydrogen atom of NAD^+ include Tyr97, Ser170, and Arg172. Mutation of these residues to other residues did not induce total inactivation [32]. Although the substrate BV may bind near this site, the exact BV binding site and mode are unknown.

BVR derived from cyanobacteria of *Synechocystis* sp. PCC 6803 (Syn BVR) was crystallized as fine needles [116], and the crystal structure has been reported [117]. Although sequence identities between mammalian BVR and Syn BVR were as low as 20-25%, the overall folding of Syn BVR was substantially similar to that of mammalian BVRs. Molecular mechanisms governing the function of this BVR remain unclear, even though the structures of BVR and NAD^+-BVR complex are known.

The crystal structures of Syn BVR in complex with $NADP^+$ and with the $NADP^+$-substrate BV (Fig. **8**) have provided significant insight into the reaction mechanisms of these enzymes [117]. Two BV

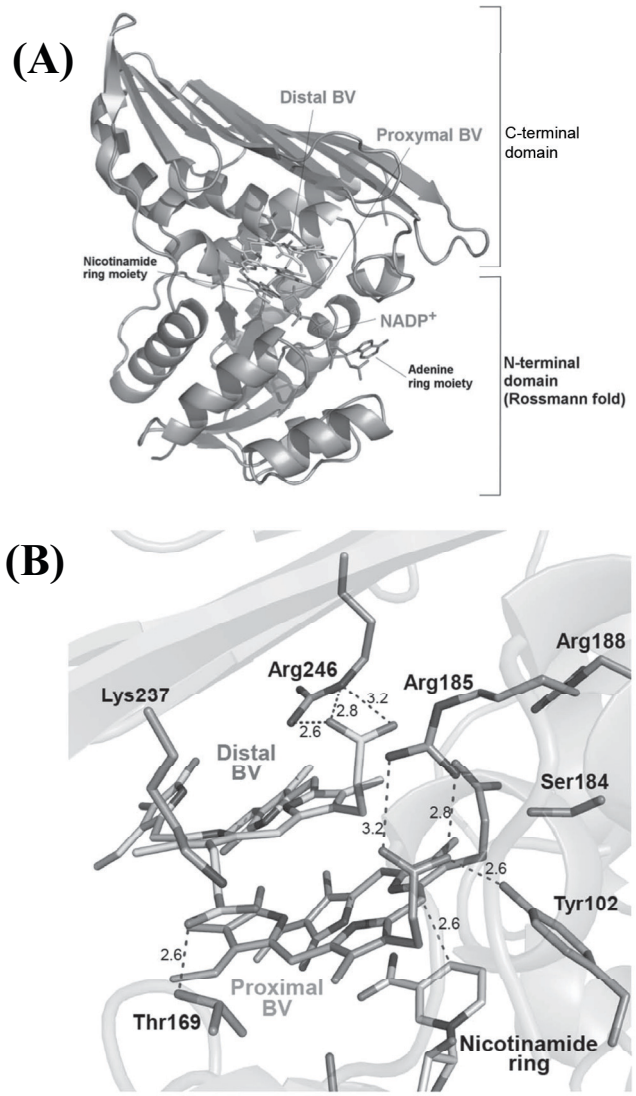

Fig. (8). The structure of Syn BVR in complex with $NADP^+$ and substrate BV. (**A**) Overall structure of the Syn BVR complex. The bound BVs and $NADP^+$ are depicted by stick model. (**B**). Close-up view of bound BVs in Syn BVR. (*A higher resolution / colour version of this figure is available in the electronic copy of the article*).

molecules, the proximal and distal BVs, bind with a stacked geometry at the active site (Fig. **8B**). To the best of our knowledge, parallel stacking of two tetrapyrrole molecules is a rare binding configuration. In this structure, the nicotinamide ring of $NADP^+$ is located near the reaction site of the proximal BV (C10 position). This structure is appropriate for hydride transfer from NADPH to the C10 atom of the proximal BV. One of the functions of the distal BV seems to include stabilizing the positions of the proximal BV and NADPH to promote hydride transfer.

Steady-state kinetics reveals likely catalytic residues. Turnover rates were dramatically decreased rela-

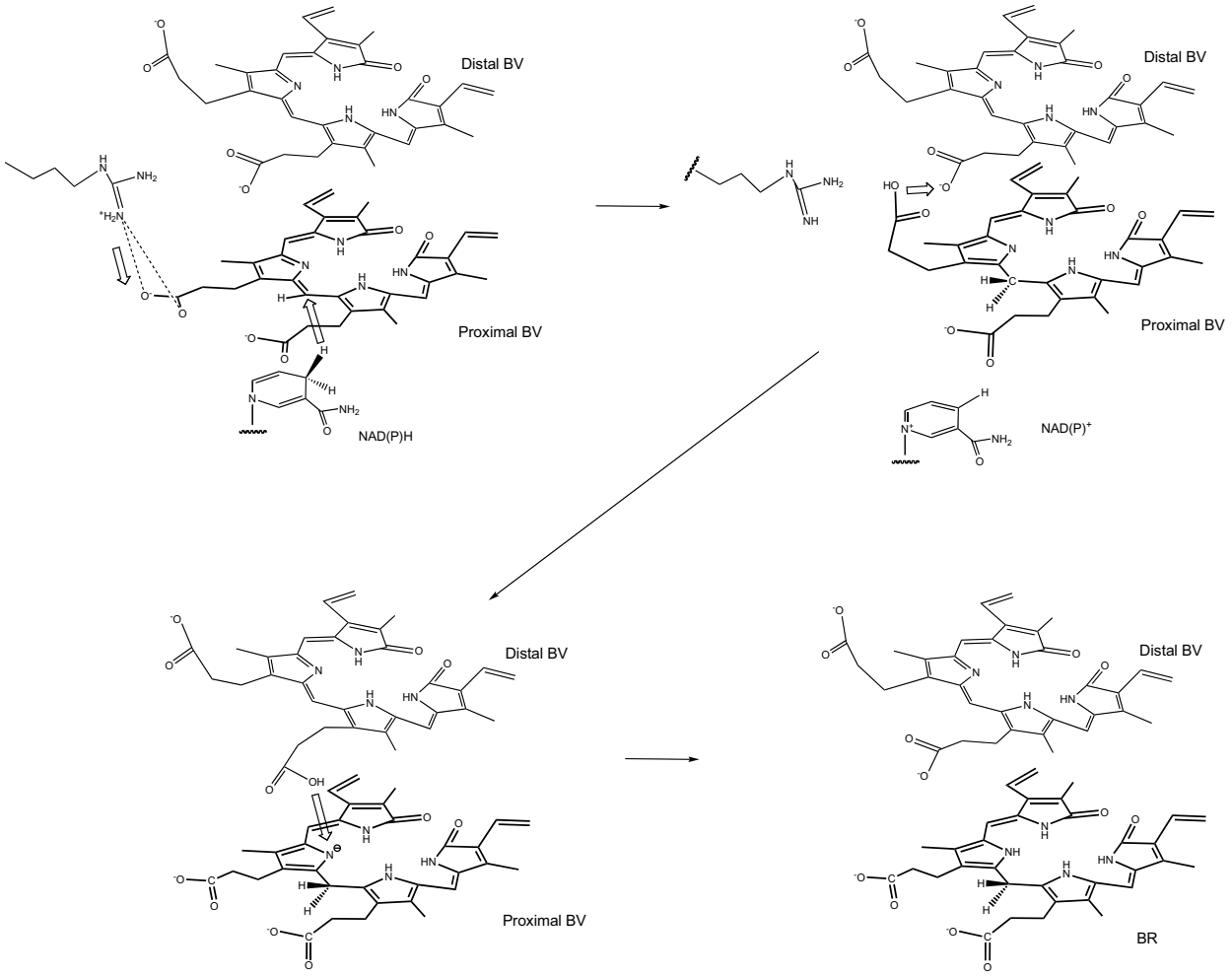

Fig. (9). Proposed mechanism of the BVR reaction. The filled and open arrows indicate hydride and proton transfer, respectively. A hydride from NAD(P)H is directly transferred to the C10 double bond of the proximal BV, initiating the reduction of proximal BV. The propionate side chain of proximal BV accepts a proton from Arg185, thereby abolishing the electrostatic interaction between Arg185 and propionate and increasing the flexibility of the side chain. Subsequently, the proton is transferred to the propionate side chain in distal BV, and the protonated propionic acid group in the distal BV moves toward the reducing site to transfer the proton. Finally, the proximal BV accepts the proton to produce BR.

tive to those of wild-type protein through the introduction of mutations at Arg185 (R185A and R185K) in Syn BVR. These mutations did not significantly alter the affinity for these enzymes for substrate (K_m). R172E and R172K mutations introduced into human BVR completely abolished enzymatic activity, and the k_{cat}/K_m values in rat BVR were remarkably decreased by introducing the corresponding mutation (R171). These data indicate that this arginine residue is the common catalytic residue of BVRs. A reaction mechanism involving the arginine residue and the propionate group of the distal BV has been proposed (Fig. **9**).

3.2. New Functions of BVR

Recent studies have established new functions for BVR, one of which is DNA binding ability. Maines group reported that human BVR binds to the promoter region of HO-1 (called AP-1 site) [118] and to the ATF-2 promoter (ATF-2 is a transcription factor for the activation of cAMP Response Element (CRE)) [29]. These promoter regions exhibit a similar sequence (TGTAGTCA). Therefore, it is feasible that human BVR functions in cell signaling by modulating HO-1 and ATF-2 expression.

Another uncovered feature of BVR is its function as a serine/threonine kinase [119]. BVR kinase activity is promoted by oxygen radicals, and activity of this enzyme in response to cGMP and oxidative stress is concomitant with BVR translocation into the nucleus [118, 120]. The amino acid sequence of BVR contains a bZip-like motif, which is commonly found in activators that are regulated in response to cellular signaling.

Taken together, these observations establish BVR as a multi-functional enzyme; however, the molecular mechanisms underlying functions such as BV reduction, DNA binding, and kinase activity remain unclear. Further studies are required to definitively establish the exact physiological role of BVR.

CONCLUSION

In summary, HO and BVR are indispensable for heme metabolism. This system is critical for the recycling of iron, and it also functions to protect cells from anti-oxidative stress and to supply CO as a signal transducer. In the last few decades, physiological, biochemical, spectroscopic, and crystallographic studies of the HO reaction, including the discrimination mechanism for CO and O_2, have been performed. The complex structure of CPR and heme-HO reveals the mechanism underlying electron transfers from CPR to heme-HO. Based on the HO structural analysis, several HO inhibitors have been developed. Recently a ternary complex of $NADP^+$-BV-BVR structure was determined. This structure may also contribute to the development of BVR inhibitors.

LIST OF ABBREVIATIONS

HO	=	Heme Oxygenase
BV	=	Biliverdin
CPR	=	NADPH-cytochrome P450 Oxidoreductase
BR	=	Bilirubin
BVR	=	Biliverdin Reductase
CD-loop	=	A Surface-exposed Loop Between C and D-helices in Rat HO-1
HRM	=	Heme Regulatory Motif
O_2	=	Oxygen Molecule
CO	=	Carbon Monoxide
Syn HO-1	=	HO-1 from *Synechocystis* sp. PCC 6803
Syn HO-2	=	HO-2 from *Synechocystis* sp. PCC 6803
EPR	=	Electron Paramagnetic Resonance
NMR	=	Nuclear Magnetic Resonance
ENDOR	=	Electron Nuclear Double Resonance
FMN	=	Flavin Mononucleotide
FAD	=	Flavin Adenine Dinucleotide
NADPH	=	Nicotinamide Adenine Dinucleotide Phosphate
ΔTGEE	=	The Open form Stabilized rat CPR Mutant
DIOCPI	=	2-[2-(4-chlorophenyl)ethyl]-2-[(1*H*-imidazole-1-yl)methyl]-1,3-dioxolane
DTT	=	Dithiothreitol
DTE	=	Dithioerythritol
HmuO	=	HO from *Corynebacterium diphtheriae*
NADH	=	Nicotinamide Adenine Dinucleotide
NAD^+	=	Oxidized form of NADH
$NADP^+$	=	Oxidized form of NADPH
BvdR	=	Cyanobacterial Mammalian BVR Homolog
Syn BVR	=	BvdR from *Synechocystis* sp. PCC 6803

CONSENT FOR PUBLICATION

Not applicable.

FUNDING

This work has financially been supported by Grants-in-Aid for Scientific Research (Grant Numbers 20770092, 25840026, 19K06515 to Masakazu Sugishima, Grant Numbers 20H03196 to Kei Wada, Grant Numbers 16570095,18570105, 20370037, 23370052 to Keiichi Fukuyama) from MEXT and JSPS, and grants from the Ishibashi Foundation for the Promotion of Science (to Masakazu Sugishima), the Pharmacological Research Foundation Tokyo (to Kei Wada), JST-Mirai Program (to Kei Wada), and Takeda Science Foundation (to Masakazu Sugishima and Kei Wada).

CONFLICT OF INTEREST

The authors declare no conflict of interest, financial or otherwise.

ACKNOWLEDGEMENTS

The synchrotron radiation experiments were performed on BL32XU, BL38B1, BL41XU, BL44B2, and BL44XU at SPring-8 (Sayo, Hyogo, Japan) and BioCARS at APS (Argonne, IL, USA). This research was also partially supported by the Platform Project for Supporting Drug Discovery and Life Science Research (BINDS). We thank all the beamline staff for their as-

sistance with data collection. We also thank Drs. M. Noguchi, Y. Omata, H. Sakamoto, Y. Higashimoto, H. Sato, S. Hayashi, J. Harada, K. Moffat, V. Šrajer, Y. Mizutani, K. Sugase, E. Harada, Y. Hagiwara, and M. Unno for their active contributions to experiments and helpful discussions.

REFERENCES

[1] Tenhunen, R.; Marver, H.S.; Schmid, R. The enzymatic conversion of heme to bilirubin by microsomal heme oxygenase. *Proc. Natl. Acad. Sci. USA,* **1968**, *61*(2), 748-755. http://dx.doi.org/10.1073/pnas.61.2.748 PMID: 4386763

[2] Tenhunen, R.; Marver, H.S.; Schmid, R. Microsomal heme oxygenase. Characterization of the enzyme. *J. Biol. Chem.,* **1969**, *244*(23), 6388-6394. PMID: 4390967

[3] Ryter, S.W.; Otterbein, L.E.; Morse, D.; Choi, A.M. Heme oxygenase/carbon monoxide signaling pathways: regulation and functional significance. *Mol. Cell. Biochem.,* **2002**, *234-235*(1-2), 249-263. http://dx.doi.org/10.1023/A:1015957026924 PMID: 12162441

[4] Morikawa, T.; Kajimura, M.; Nakamura, T.; Hishiki, T.; Nakanishi, T.; Yukutake, Y.; Nagahata, Y.; Ishikawa, M.; Hattori, K.; Takenouchi, T.; Takahashi, T.; Ishii, I.; Matsubara, K.; Kabe, Y.; Uchiyama, S.; Nagata, E.; Gadalla, M.M.; Snyder, S.H.; Suematsu, M. Hypoxic regulation of the cerebral microcirculation is mediated by a carbon monoxide-sensitive hydrogen sulfide pathway. *Proc. Natl. Acad. Sci. USA,* **2012**, *109*(4), 1293-1298. http://dx.doi.org/10.1073/pnas.1119658109 PMID: 22232681

[5] Shintani, T.; Iwabuchi, T.; Soga, T.; Kato, Y.; Yamamoto, T.; Takano, N.; Hishiki, T.; Ueno, Y.; Ikeda, S.; Sakuragawa, T.; Ishikawa, K.; Goda, N.; Kitagawa, Y.; Kajimura, M.; Matsumoto, K.; Suematsu, M. Cystathionine beta-synthase as a carbon monoxide-sensitive regulator of bile excretion. *Hepatology,* **2009**, *49*(1), 141-150. http://dx.doi.org/10.1002/hep.22604 PMID: 19085910

[6] Dioum, E.M.; Rutter, J.; Tuckerman, J.R.; Gonzalez, G.; Gilles-Gonzalez, M.A.; McKnight, S.L. NPAS2: a gas-responsive transcription factor. *Science,* **2002**, *298*(5602), 2385-2387. http://dx.doi.org/10.1126/science.1078456 PMID: 12446832

[7] Terry, M.J.; Linley, P.J.; Kohchi, T. Making light of it: the role of plant haem oxygenases in phytochrome chromophore synthesis. *Biochem. Soc. Trans.,* **2002**, *30*(4), 604-609. http://dx.doi.org/10.1042/bst0300604 PMID: 12196146

[8] Pendrak, M.L.; Chao, M.P.; Yan, S.S.; Roberts, D.D. Heme oxygenase in Candida albicans is regulated by hemoglobin and is necessary for metabolism of exogenous heme and hemoglobin to alpha-biliverdin. *J. Biol. Chem.,* **2004**, *279*(5), 3426-3433. http://dx.doi.org/10.1074/jbc.M311550200 PMID: 14615478

[9] Frankenberg-Dinkel, N. Bacterial heme oxygenases. *Antioxid. Redox Signal.,* **2004**, *6*(5), 825-834. PMID: 15345142

[10] Kikuchi, G.; Yoshida, T. Heme catabolism by the reconstituted heme oxygenase system. *Ann. Clin. Res.,* **1976**, *8*(Suppl. 17), 10-17. PMID: 827230

[11] Kikuchi, G.; Yoshida, T. Function and induction of the microsomal heme oxygenase. *Mol. Cell. Biochem.,* **1983**, *53-54*(1-2), 163-183. http://dx.doi.org/10.1007/BF00225252 PMID: 6353193

[12] Kikuchi, G.; Yoshida, T.; Noguchi, M. Heme oxygenase and heme degradation. *Biochem. Biophys. Res. Commun.,* **2005**, *338*(1), 558-567. http://dx.doi.org/10.1016/j.bbrc.2005.08.020 PMID: 16115609

[13] Huber, W.J., III; Backes, W.L. Expression and characterization of full-length human heme oxygenase-1: the presence of intact membrane-binding region leads to increased binding affinity for NADPH cytochrome P450 reductase. *Biochemistry,* **2007**, *46*(43), 12212-12219. http://dx.doi.org/10.1021/bi701496z PMID: 17915953

[14] Huber, W.J., III; Marohnic, C.C.; Peters, M.; Alam, J.; Reed, J.R.; Masters, B.S.; Backes, W.L. Measurement of membrane-bound human heme oxygenase-1 activity using a chemically defined assay system. *Drug Metab. Dispos.,* **2009**, *37*(4), 857-864. http://dx.doi.org/10.1124/dmd.108.025023 PMID: 19131520

[15] Wilks, A.; Black, S.M.; Miller, W.L.; Ortiz de Montellano, P.R. Expression and characterization of truncated human heme oxygenase (hHO-1) and a fusion protein of hHO-1 with human cytochrome P450 reductase. *Biochemistry,* **1995**, *34*(13), 4421-4427. http://dx.doi.org/10.1021/bi00013a034 PMID: 7703255

[16] Wilks, A.; Ortiz de Montellano, P.R. Rat liver heme oxygenase. High level expression of a truncated soluble form and nature of the meso-hydroxylating species. *J. Biol. Chem.,* **1993**, *268*(30), 22357-22362. PMID: 8226746

[17] Beale, S.I. Biosynthesis of Phycobilins. *Chem. Rev.,* **1993**, *93*, 785-802. http://dx.doi.org/10.1021/cr00018a008

[18] Rockwell, N.C.; Su, Y.S.; Lagarias, J.C. Phytochrome structure and signaling mechanisms. *Annu. Rev. Plant Biol.,* **2006**, *57*, 837-858. http://dx.doi.org/10.1146/annurev.arplant.56.032604.144208 PMID: 16669784

[19] Frankenberg, N.; Lagarias, J.C. Biosynthesis and biological functions of bilins in: *The Porphyrin Handbook*; Kadish, K.M.; Smith, K.M.; Guilard, R., Eds.; Academic Press: San Diego, **2003**, pp. 211-235. https://doi.org/10.1016/B978-0-08-092387-1.50013-8

[20] Kohchi, T.; Mukougawa, K.; Frankenberg, N.; Masuda, M.; Yokota, A.; Lagarias, J.C. The Arabidopsis HY2 gene encodes phytochromobilin synthase, a ferredoxin-dependent biliverdin reductase. *Plant Cell,* **2001**, *13*(2), 425-436. http://dx.doi.org/10.1105/tpc.13.2.425 PMID: 11226195

[21] Dammeyer, T.; Frankenberg-Dinkel, N. Function and distribution of bilin biosynthesis enzymes in photosynthetic organisms. *Photochem. Photobiol. Sci.,* **2008**, *7*(10), 1121-1130. http://dx.doi.org/10.1039/b807209b PMID: 18846276

[22] Ikeuchi, M.; Ishizuka, T. Cyanobacteriochromes: a new superfamily of tetrapyrrole-binding photoreceptors in cyanobacteria. *Photochem. Photobiol. Sci.,* **2008**, *7*(10), 1159-1167. http://dx.doi.org/10.1039/b802660m PMID: 18846279

[23] Chen, Y.R.; Su, Y.S.; Tu, S.L. Distinct phytochrome actions in nonvascular plants revealed by targeted inactivation of phytobilin biosynthesis. *Proc. Natl. Acad. Sci. USA,* **2012**, *109*(21), 8310-8315.

http://dx.doi.org/10.1073/pnas.1201744109 PMID: 22566621

[24] Singleton, J.W.; Laster, L. Biliverdin reductase of guinea pig liver. *J. Biol. Chem.,* **1965**, *240*(12), 4780-4789. PMID: 4378982

[25] Baranano, D.E.; Rao, M.; Ferris, C.D.; Snyder, S.H. Biliverdin reductase: a major physiologic cytoprotectant. *Proc. Natl. Acad. Sci. USA,* **2002**, *99*(25), 16093-16098. http://dx.doi.org/10.1073/pnas.252626999 PMID: 12456881

[26] Stocker, R.; Yamamoto, Y.; McDonagh, A.F.; Glazer, A.N.; Ames, B.N. Bilirubin is an antioxidant of possible physiological importance. *Science,* **1987**, *235*(4792), 1043-1046. http://dx.doi.org/10.1126/science.3029864 PMID: 3029864

[27] McDonagh, A.F.; Palma, L.A.; Lightner, D.A. Blue light and bilirubin excretion. *Science,* **1980**, *208*(4440), 145-151. http://dx.doi.org/10.1126/science.7361112 PMID: 7361112

[28] Lerner-Marmarosh, N.; Shen, J.; Torno, M.D.; Kravets, A.; Hu, Z.; Maines, M.D. Human biliverdin reductase: a member of the insulin receptor substrate family with serine/threonine/tyrosine kinase activity. *Proc. Natl. Acad. Sci. USA,* **2005**, *102*(20), 7109-7114. http://dx.doi.org/10.1073/pnas.0502173102 PMID: 15870194

[29] Kravets, A.; Hu, Z.; Miralem, T.; Torno, M.D.; Maines, M.D. Biliverdin reductase, a novel regulator for induction of activating transcription factor-2 and heme oxygenase-1. *J. Biol. Chem.,* **2004**, *279*(19), 19916-19923. http://dx.doi.org/10.1074/jbc.M314251200 PMID: 14988408

[30] Schluchter, W.M.; Glazer, A.N. Characterization of cyanobacterial biliverdin reductase. Conversion of biliverdin to bilirubin is important for normal phycobiliprotein biosynthesis. *J. Biol. Chem.,* **1997**, *272*(21), 13562-13569. http://dx.doi.org/10.1074/jbc.272.21.13562 PMID: 9153203

[31] Kikuchi, A.; Park, S.Y.; Miyatake, H.; Sun, D.; Sato, M.; Yoshida, T.; Shiro, Y. Crystal structure of rat biliverdin reductase. *Nat. Struct. Biol.,* **2001**, *8*(3), 221-225. http://dx.doi.org/10.1038/84955 PMID: 11224565

[32] Whitby, F.G.; Phillips, J.D.; Hill, C.P.; McCoubrey, W.; Maines, M.D. Crystal structure of a biliverdin IXalpha reductase enzyme-cofactor complex. *J. Mol. Biol.,* **2002**, *319*(5), 1199-1210. http://dx.doi.org/10.1016/S0022-2836(02)00383-2 PMID: 12079357

[33] Kikuchi, G.; Yoshida, T. Heme degradation by the microsomal heme oxygenase system. *Trends Biochem. Sci.,* **1980**, *5*, 323-325. http://dx.doi.org/10.1016/0968-0004(80)90141-3

[34] Montellano, P.R. The mechanism of heme oxygenase. *Curr. Opin. Chem. Biol.,* **2000**, *4*(2), 221-227. http://dx.doi.org/10.1016/S1367-5931(99)00079-4 PMID: 10742194

[35] Yoshida, T.; Migita, C.T. Mechanism of heme degradation by heme oxygenase. *J. Inorg. Biochem.,* **2000**, *82*(1-4), 33-41. http://dx.doi.org/10.1016/S0162-0134(00)00156-2 PMID: 11132636

[36] Matsui, T.; Unno, M.; Ikeda-Saito, M. Heme oxygenase reveals its strategy for catalyzing three successive oxygenation reactions. *Acc. Chem. Res.,* **2010**, *43*(2), 240-247. http://dx.doi.org/10.1021/ar9001685 PMID: 19827796

[37] Maines, M.D. Overview of heme degradation pathway. *Curr. Protoc. Toxicol.,* **2001** *Chapter 9*(Unit 9). http://dx.doi.org/10.1002/0471140856.tx0901s00

[38] Stocker, R. Antioxidant activities of bile pigments. *Antioxid. Redox Signal.,* **2004**, *6*(5), 841-849. PMID: 15345144

[39] Florczyk, U.M.; Jozkowicz, A.; Dulak, J. Biliverdin reductase: new features of an old enzyme and its potential therapeutic significance. *Pharmacol. Rep.,* **2008**, *60*(1), 38-48. PMID: 18276984

[40] Hwang, H.W.; Lee, J.R.; Chou, K.Y.; Suen, C.S.; Hwang, M.J.; Chen, C.; Shieh, R.C.; Chau, L.Y. Oligomerization is crucial for the stability and function of heme oxygenase-1 in the endoplasmic reticulum. *J. Biol. Chem.,* **2009**, *284*(34), 22672-22679. http://dx.doi.org/10.1074/jbc.M109.028001 PMID: 19556236

[41] Abraham, N.G.; Drummond, G.S.; Lutton, J.D.; Kappas, A. The biological significance and physiological role of heme oxygenase. *Cell. Physiol. Biochem.,* **1996**, *6*, 129-168. http://dx.doi.org/10.1159/000154819

[42] Yoshida, T.; Noguchi, M.; Kikuchi, G. Oxygenated form of heme. heme oxygenase complex and requirement for second electron to initiate heme degradation from the oxygenated complex. *J. Biol. Chem.,* **1980**, *255*(10), 4418-4420. PMID: 6892813

[43] Sun, J.; Wilks, A.; Ortiz de Montellano, P.R.; Loehr, T.M. Resonance Raman and EPR spectroscopic studies on heme-heme oxygenase complexes. *Biochemistry,* **1993**, *32*(51), 14151-14157. http://dx.doi.org/10.1021/bi00214a012 PMID: 8260499

[44] Takahashi, S.; Wang, J.; Rousseau, D.L.; Ishikawa, K.; Yoshida, T.; Host, J.R.; Ikeda-Saito, M. Heme-heme oxygenase complex. Structure of the catalytic site and its implication for oxygen activation. *J. Biol. Chem.,* **1994**, *269*(2), 1010-1014. PMID: 8288555

[45] Migita, C.T.; Matera, K.M.; Ikeda-Saito, M.; Olson, J.S.; Fujii, H.; Yoshimura, T.; Zhou, H.; Yoshida, T. The oxygen and carbon monoxide reactions of heme oxygenase. *J. Biol. Chem.,* **1998**, *273*(2), 945-949. http://dx.doi.org/10.1074/jbc.273.2.945 PMID: 9422754

[46] Zhou, H.; Migita, C.T.; Sato, M.; Sun, D.; Zhang, X.; Ikeda-Saito, M.; Fujii, H.; Yoshida, T. Participation of carboxylate amino acid side chain in regiospecific oxidation of heme by heme oxygenase. *J. Am. Chem. Soc.,* **2000**, *122*, 8311-8312. http://dx.doi.org/10.1021/ja0002868

[47] Fujii, H.; Zhang, X.; Tomita, T.; Ikeda-Saito, M.; Yoshida, T. A role for highly conserved carboxylate, aspartate-140, in oxygen activation and heme degradation by heme oxygenase-1. *J. Am. Chem. Soc.,* **2001**, *123*(27), 6475-6484. http://dx.doi.org/10.1021/ja010490a PMID: 11439033

[48] Lightning, L.K.; Huang, H.; Moenne-Loccoz, P.; Loehr, T.M.; Schuller, D.J.; Poulos, T.L.; de Montellano, P.R. Disruption of an active site hydrogen bond converts human heme oxygenase-1 into a peroxidase. *J. Biol. Chem.,* **2001**, *276*(14), 10612-10619. http://dx.doi.org/10.1074/jbc.M010349200 PMID: 11121422

[49] Schuller, D.J.; Wilks, A.; Ortiz de Montellano, P.; Poulos, T.L. Crystallization of recombinant human heme oxygenase-1. *Protein Sci.,* **1998**, *7*(8), 1836-1838. http://dx.doi.org/10.1002/pro.5560070820 PMID: 10082382

[50] Omata, Y.; Asada, S.; Sakamoto, H.; Fukuyama, K.; Noguchi, M. Crystallization and preliminary X-ray diffraction studies on the water soluble form of rat heme oxygenase-1

in complex with heme. *Acta Crystallogr. D Biol. Crystallogr.,* **1998**, *54*(Pt 5), 1017-1019. http://dx.doi.org/10.1107/S0907444998003448 PMID: 9757125

[51] Schuller, D.J.; Wilks, A.; Ortiz de Montellano, P.R.; Poulos, T.L. Crystal structure of human heme oxygenase-1. *Nat. Struct. Biol.,* **1999**, *6*(9), 860-867. http://dx.doi.org/10.1038/12319 PMID: 10467099

[52] Sugishima, M.; Omata, Y.; Kakuta, Y.; Sakamoto, H.; Noguchi, M.; Fukuyama, K. Crystal structure of rat heme oxygenase-1 in complex with heme. *FEBS Lett.,* **2000**, *471*(1), 61-66. http://dx.doi.org/10.1016/S0014-5793(00)01353-3 PMID: 10760513

[53] La Mar, G.N.; Asokan, A.; Espiritu, B.; Yeh, D.C.; Auclair, K.; Ortiz De Montellano, P.R. Solution 1H NMR of the active site of substrate-bound, cyanide-inhibited human heme oxygenase. comparison to the crystal structure of the water-ligated form. *J. Biol. Chem.,* **2001**, *276*(19), 15676-15687. http://dx.doi.org/10.1074/jbc.M009974200 PMID: 11297521

[54] Li, Y.; Syvitski, R.T.; Chu, G.C.; Ikeda-Saito, M.; La Mar, G.N. Solution 1H NMR investigation of the active site molecular and electronic structures of the substrate-bound, cyanide-inhibited HmuO, a bacterial heme oxygenase from C. diphtheriae. *J. Biol. Chem.,* **2003**, *278*(9), 6651-6663. http://dx.doi.org/10.1074/jbc.M211249200 PMID: 12480929

[55] Davydov, R.; Kofman, V.; Fujii, H.; Yoshida, T.; Ikeda-Saito, M.; Hoffman, B.M. Catalytic mechanism of heme oxygenase through EPR and ENDOR of cryoreduced oxyheme oxygenase and its Asp 140 mutants. *J. Am. Chem. Soc.,* **2002**, *124*(8), 1798-1808. http://dx.doi.org/10.1021/ja0122391 PMID: 11853459

[56] Varfaj, F.; Lampe, J.N.; Ortiz de Montellano, P.R. Role of cysteine residues in heme binding to human heme oxygenase-2 elucidated by two-dimensional NMR spectroscopy. *J. Biol. Chem.,* **2012**, *287*(42), 35181-35191. http://dx.doi.org/10.1074/jbc.M112.378042 PMID: 22923613

[57] Bianchetti, C.M.; Yi, L.; Ragsdale, S.W.; Phillips, G.N.Jr. Comparison of apo- and heme-bound crystal structures of a truncated human heme oxygenase-2. *J. Biol. Chem.,* **2007**, *282*(52), 37624-37631. http://dx.doi.org/10.1074/jbc.M707396200 PMID: 17965015

[58] Sugishima, M.; Sakamoto, H.; Kakuta, Y.; Omata, Y.; Hayashi, S.; Noguchi, M.; Fukuyama, K. Crystal structure of rat apo-heme oxygenase-1 (HO-1): mechanism of heme binding in HO-1 inferred from structural comparison of the apo and heme complex forms. *Biochemistry,* **2002**, *41*(23), 7293-7300. http://dx.doi.org/10.1021/bi025662a PMID: 12044160

[59] Lad, L.; Schuller, D.J.; Shimizu, H.; Friedman, J.; Li, H.; Ortiz de Montellano, P.R.; Poulos, T.L. Comparison of the heme-free and -bound crystal structures of human heme oxygenase-1. *J. Biol. Chem.,* **2003**, *278*(10), 7834-7843. http://dx.doi.org/10.1074/jbc.M211450200 PMID: 12500973

[60] Unno, M.; Ardèvol, A.; Rovira, C.; Ikeda-Saito, M. Structures of the substrate-free and product-bound forms of HmuO, a heme oxygenase from corynebacterium diphtheriae: x-ray crystallography and molecular dynamics investigation. *J. Biol. Chem.,* **2013**, *288*(48), 34443-34458. http://dx.doi.org/10.1074/jbc.M113.486936 PMID: 24106279

[61] Harada, E.; Sugishima, M.; Harada, J.; Fukuyama, K.; Sugase, K. Distal regulation of heme binding of heme oxygenase-1 mediated by conformational fluctuations. *Biochemistry,* **2015**, *54*(2), 340-348. http://dx.doi.org/10.1021/bi5009694 PMID: 25496210

[62] Sugishima, M.; Moffat, K.; Noguchi, M. Discrimination between CO and O_2) in heme oxygenase: comparison of static structures and dynamic conformation changes following CO photolysis. *Biochemistry,* **2012**, *51*(43), 8554-8562. http://dx.doi.org/10.1021/bi301175x PMID: 23043644

[63] Takahashi, S.; Ishikawa, K.; Takeuchi, N.; Ikeda-Saito, M.; Yoshida, T.; Rousseau, D.L. Oxygen-bound heme-heme oxygenase complex: evidence for a highly bent structure of the cooridnated oxygen. *J. Am. Chem. Soc.,* **1995**, *117*, 6002-6006. http://dx.doi.org/10.1021/ja00127a013

[64] Unno, M.; Matsui, T.; Chu, G.C.; Couture, M.; Yoshida, T.; Rousseau, D.L.; Olson, J.S.; Ikeda-Saito, M. Crystal structure of the dioxygen-bound heme oxygenase from *Corynebacterium diphtheriae*: implications for heme oxygenase function. *J. Biol. Chem.,* **2004**, *279*(20), 21055-21061. http://dx.doi.org/10.1074/jbc.M400491200 PMID: 14966119

[65] Sugishima, M.; Sakamoto, H.; Noguchi, M.; Fukuyama, K. Crystal structures of ferrous and CO-, $CN^{(-)}$, and NO-bound forms of rat heme oxygenase-1 (HO-1) in complex with heme: structural implications for discrimination between CO and O_2 in HO-1. *Biochemistry,* **2003**, *42*(33), 9898-9905. http://dx.doi.org/10.1021/bi027268i PMID: 12924938

[66] Sugishima, M.; Sakamoto, H.; Higashimoto, Y.; Omata, Y.; Hayashi, S.; Noguchi, M.; Fukuyama, K. Crystal structure of rat heme oxygenase-1 in complex with heme bound to azide. Implication for regiospecific hydroxylation of heme at the alpha-meso carbon. *J. Biol. Chem.,* **2002**, *277*(47), 45086-45090. http://dx.doi.org/10.1074/jbc.M207267200 PMID: 12235152

[67] Yamaoka, M.; Sugishima, M.; Noguchi, M.; Fukuyama, K.; Mizutani, Y. Protein dynamics of heme–heme oxygenase-1 complex following carbon monoxide dissociation. *J. Raman Spectrosc.,* **2011**, *42*, 910-916. http://dx.doi.org/10.1002/jrs.2797

[68] Friedman, J.; Meharenna, Y.T.; Wilks, A.; Poulos, T.L. Diatomic ligand discrimination by the heme oxygenases from *Neisseria meningitidis* and *Pseudomonas aeruginosa. J. Biol. Chem.,* **2007**, *282*(2), 1066-1071. http://dx.doi.org/10.1074/jbc.M609112200 PMID: 17095508

[69] Sugishima, M.; Sakamoto, H.; Noguchi, M.; Fukuyama, K. CO-trapping site in heme oxygenase revealed by photolysis of its co-bound heme complex: mechanism of escaping from product inhibition. *J. Mol. Biol.,* **2004**, *341*(1), 7-13. http://dx.doi.org/10.1016/j.jmb.2004.05.048 PMID: 15312758

[70] Sakamoto, H.; Omata, Y.; Hayashi, S.; Harada, S.; Palmer, G.; Noguchi, M. The reactivity of alpha-hydroxyhaem and verdohaem bound to haem oxygenase-1 to dioxygen and sodium dithionite. *Eur. J. Biochem.,* **2002**, *269*(21), 5231-5239. http://dx.doi.org/10.1046/j.1432-1033.2002.03230.x PMID: 12392555

[71] Sakamoto, H.; Omata, Y.; Palmer, G.; Noguchi, M. Ferric alpha-hydroxyheme bound to heme oxygenase can be converted to verdoheme by dioxygen in the absence of added

reducing equivalents. *J. Biol. Chem.,* **1999**, *274*(26), 18196-18200. http://dx.doi.org/10.1074/jbc.274.26.18196 PMID: 10373419

[72] Sakamoto, H.; Takahashi, K.; Higashimoto, Y.; Harada, S.; Palmer, G.; Noguchi, M. A kinetic study of the mechanism of conversion of alpha-hydroxyheme to verdoheme while bound to heme oxygenase. *Biochem. Biophys. Res. Commun.,* **2005**, *338*(1), 578-583. http://dx.doi.org/10.1016/j.bbrc.2005.08.176 PMID: 16154530

[73] Matsui, T.; Nakajima, A.; Fujii, H.; Matera, K.M.; Migita, C.T.; Yoshida, T.; Ikeda-Saito, M. O(2)- and H(2)O(2)-dependent verdoheme degradation by heme oxygenase: reaction mechanisms and potential physiological roles of the dual pathway degradation. *J. Biol. Chem.,* **2005**, *280*(44), 36833-36840. http://dx.doi.org/10.1074/jbc.M503529200 PMID: 16115896

[74] Sato, H.; Higashimoto, Y.; Sakamoto, H.; Sugishima, M.; Shimokawa, C.; Harada, J.; Palmer, G.; Noguchi, M. Reduction of oxaporphyrin ring of CO-bound α-verdoheme complexed with heme oxygenase-1 by NADPH-cytochrome P450 reductase. *J. Inorg. Biochem.,* **2011**, *105*(2), 289-296. http://dx.doi.org/10.1016/j.jinorgbio.2010.11.010 PMID: 21194630

[75] Lad, L.; Ortiz de Montellano, P.R.; Poulos, T.L. Crystal structures of ferrous and ferrous-NO forms of verdoheme in a complex with human heme oxygenase-1: catalytic implications for heme cleavage. *J. Inorg. Biochem.,* **2004**, *98*(11), 1686-1695. http://dx.doi.org/10.1016/j.jinorgbio.2004.07.004 PMID: 15522396

[76] Sugishima, M.; Sakamoto, H.; Higashimoto, Y.; Noguchi, M.; Fukuyama, K. Crystal structure of rat heme oxygenase-1 in complex with biliverdin-iron chelate. Conformational change of the distal helix during the heme cleavage reaction. *J. Biol. Chem.,* **2003**, *278*(34), 32352-32358. http://dx.doi.org/10.1074/jbc.M303682200 PMID: 12794075

[77] Wang, M.; Roberts, D.L.; Paschke, R.; Shea, T.M.; Masters, B.S.; Kim, J.J. Three-dimensional structure of NADPH-cytochrome P450 reductase: prototype for FMN- and FAD-containing enzymes. *Proc. Natl. Acad. Sci. USA,* **1997**, *94*(16), 8411-8416. http://dx.doi.org/10.1073/pnas.94.16.8411 PMID: 9237990

[78] Xia, C.; Hamdane, D.; Shen, A.L.; Choi, V.; Kasper, C.B.; Pearl, N.M.; Zhang, H.; Im, S.C.; Waskell, L.; Kim, J.J. Conformational changes of NADPH-cytochrome P450 oxidoreductase are essential for catalysis and cofactor binding. *J. Biol. Chem.,* **2011**, *286*(18), 16246-16260. http://dx.doi.org/10.1074/jbc.M111.230532 PMID: 21345800

[79] Huang, W.C.; Ellis, J.; Moody, P.C.; Raven, E.L.; Roberts, G.C. Redox-linked domain movements in the catalytic cycle of cytochrome p450 reductase. *Structure,* **2013**, *21*(9), 1581-1589. http://dx.doi.org/10.1016/j.str.2013.06.022 PMID: 23911089

[80] Pudney, C.R.; Khara, B.; Johannissen, L.O.; Scrutton, N.S. Coupled motions direct electrons along human microsomal P450 Chains. *PLoS Biol.,* **2011**, *9*(12), e1001222. http://dx.doi.org/10.1371/journal.pbio.1001222 PMID: 22205878

[81] Jenner, M.; Ellis, J.; Huang, W.C.; Lloyd Raven, E.; Roberts, G.C.; Oldham, N.J. Detection of a protein conformational equilibrium by electrospray ionisation-ion mobility-mass spectrometry. *Angew. Chem. Int. Ed. Engl.,* **2011**, *50*(36), 8291-8294. http://dx.doi.org/10.1002/anie.201101077 PMID: 21688358

[82] Hamdane, D.; Xia, C.; Im, S.C.; Zhang, H.; Kim, J.J.; Waskell, L. Structure and function of an NADPH-cytochrome P450 oxidoreductase in an open conformation capable of reducing cytochrome P450. *J. Biol. Chem.,* **2009**, *284*(17), 11374-11384. http://dx.doi.org/10.1074/jbc.M807868200 PMID: 19171935

[83] Sugishima, M.; Sato, H.; Higashimoto, Y.; Harada, J.; Wada, K.; Fukuyama, K.; Noguchi, M. Structural basis for the electron transfer from an open form of NADPH-cytochrome P450 oxidoreductase to heme oxygenase. *Proc. Natl. Acad. Sci. USA,* **2014**, *111*(7), 2524-2529. http://dx.doi.org/10.1073/pnas.1322034111 PMID: 24550278

[84] Higashimoto, Y.; Sakamoto, H.; Hayashi, S.; Sugishima, M.; Fukuyama, K.; Palmer, G.; Noguchi, M. Involvement of NADPH in the interaction between heme oxygenase-1 and cytochrome P450 reductase. *J. Biol. Chem.,* **2005**, *280*(1), 729-737. http://dx.doi.org/10.1074/jbc.M406203200 PMID: 15516695

[85] Higashimoto, Y.; Sugishima, M.; Sato, H.; Sakamoto, H.; Fukuyama, K.; Palmer, G.; Noguchi, M. Mass spectrometric identification of lysine residues of heme oxygenase-1 that are involved in its interaction with NADPH-cytochrome P450 reductase. *Biochem. Biophys. Res. Commun.,* **2008**, *367*(4), 852-858. http://dx.doi.org/10.1016/j.bbrc.2008.01.016 PMID: 18194664

[86] Higashimoto, Y.; Sato, H.; Sakamoto, H.; Takahashi, K.; Palmer, G.; Noguchi, M. The reactions of heme- and verdoheme-heme oxygenase-1 complexes with FMN-depleted NADPH-cytochrome P450 reductase. Electrons required for verdoheme oxidation can be transferred through a pathway not involving FMN. *J. Biol. Chem.,* **2006**, *281*(42), 31659-31667. http://dx.doi.org/10.1074/jbc.M606163200 PMID: 16928691

[87] Fukuyama, K. Structure and function of plant-type ferredoxins. *Photosynth. Res.,* **2004**, *81*(3), 289-301. http://dx.doi.org/10.1023/B:PRES.0000036882.19322.0a PMID: 16034533

[88] Aoki, R.; Goto, T.; Fujita, Y. A heme oxygenase isoform is essential for aerobic growth in the cyanobacterium *Synechocystis* sp. PCC 6803: modes of differential operation of two isoforms/enzymes to adapt to low oxygen environments in cyanobacteria. *Plant Cell Physiol.,* **2011**, *52*(10), 1744-1756. http://dx.doi.org/10.1093/pcp/pcr108 PMID: 21828104

[89] Cornejo, J.; Beale, S.I. Phycobilin biosynthetic reactions in extracts of cyanobacteria. *Photosynth. Res.,* **1997**, *51*, 223-230. http://dx.doi.org/10.1023/A:1005855010560

[90] Cornejo, J.; Willows, R.D.; Beale, S.I. Phytobilin biosynthesis: cloning and expression of a gene encoding soluble ferredoxin-dependent heme oxygenase from *Synechocystis* sp. PCC 6803. *Plant J.,* **1998**, *15*(1), 99-107. http://dx.doi.org/10.1046/j.1365-313X.1998.00186.x PMID: 9744099

[91] Sugishima, M.; Hagiwara, Y.; Zhang, X.; Yoshida, T.; Migita, C.T.; Fukuyama, K. Crystal structure of dimeric heme oxygenase-2 from *Synechocystis* sp. PCC 6803 in complex with heme. *Biochemistry,* **2005**, *44*(11), 4257-4266.
http://dx.doi.org/10.1021/bi0480483 PMID: 15766254

[92] Sugishima, M.; Migita, C.T.; Zhang, X.; Yoshida, T.; Fukuyama, K. Crystal structure of heme oxygenase-1 from cyanobacterium *Synechocystis* sp. PCC 6803 in complex with heme. *Eur. J. Biochem.,* **2004**, *271*(22), 4517-4525.
http://dx.doi.org/10.1111/j.1432-1033.2004.04411.x PMID: 15560792

[93] Schuller, D.J.; Zhu, W.; Stojiljkovic, I.; Wilks, A.; Poulos, T.L. Crystal structure of heme oxygenase from the gram-negative pathogen *Neisseria meningitidis* and a comparison with mammalian heme oxygenase-1. *Biochemistry,* **2001**, *40*(38), 11552-11558.
http://dx.doi.org/10.1021/bi0110239 PMID: 11560504

[94] Hirotsu, S.; Chu, G.C.; Unno, M.; Lee, D.S.; Yoshida, T.; Park, S.Y.; Shiro, Y.; Ikeda-Saito, M. The crystal structures of the ferric and ferrous forms of the heme complex of HmuO, a heme oxygenase of *Corynebacterium diphtheriae*. *J. Biol. Chem.,* **2004**, *279*(12), 11937-11947.
http://dx.doi.org/10.1074/jbc.M311631200 PMID: 14645223

[95] Friedman, J.; Lad, L.; Li, H.; Wilks, A.; Poulos, T.L. Structural basis for novel delta-regioselective heme oxygenation in the opportunistic pathogen *Pseudomonas aeruginosa*. *Biochemistry,* **2004**, *43*(18), 5239-5245.
http://dx.doi.org/10.1021/bi049687g PMID: 15122889

[96] Unno, M.; Matsui, T.; Ikeda-Saito, M. Structure and catalytic mechanism of heme oxygenase. *Nat. Prod. Rep.,* **2007**, *24*(3), 553-570.
http://dx.doi.org/10.1039/b604180a PMID: 17534530

[97] Unno, M.; Matsui, T.; Ikeda-Saito, M. Crystallographic studies of heme oxygenase complexed with an unstable reaction intermediate, verdoheme. *J. Inorg. Biochem.,* **2012**, *113*, 102-109.
http://dx.doi.org/10.1016/j.jinorgbio.2012.04.012 PMID: 22673156

[98] Maines, M.D. Zinc. protoporphyrin is a selective inhibitor of heme oxygenase activity in the neonatal rat. *Biochim. Biophys. Acta,* **1981**, *673*(3), 339-350.
http://dx.doi.org/10.1016/0304-4165(81)90465-7 PMID: 6894392

[99] Vlahakis, J.Z.; Kinobe, R.T.; Bowers, R.J.; Brien, J.F.; Nakatsu, K.; Szarek, W.A. Synthesis and evaluation of azalanstat analogues as heme oxygenase inhibitors. *Bioorg. Med. Chem. Lett.,* **2005**, *15*(5), 1457-1461.
http://dx.doi.org/10.1016/j.bmcl.2004.12.075 PMID: 15713406

[100] Kinobe, R.T.; Vlahakis, J.Z.; Vreman, H.J.; Stevenson, D.K.; Brien, J.F.; Szarek, W.A.; Nakatsu, K. Selectivity of imidazole-dioxolane compounds for *in vitro* inhibition of microsomal haem oxygenase isoforms. *Br. J. Pharmacol.,* **2006**, *147*(3), 307-315.
http://dx.doi.org/10.1038/sj.bjp.0706555 PMID: 16331285

[101] Vlahakis, J.Z.; Kinobe, R.T.; Bowers, R.J.; Brien, J.F.; Nakatsu, K.; Szarek, W.A. Imidazole-dioxolane compounds as isozyme-selective heme oxygenase inhibitors. *J. Med. Chem.,* **2006**, *49*(14), 4437-4441.
http://dx.doi.org/10.1021/jm0511435 PMID: 16821802

[102] Sugishima, M.; Higashimoto, Y.; Oishi, T.; Takahashi, H.; Sakamoto, H.; Noguchi, M.; Fukuyama, K. X-ray crystallographic and biochemical characterization of the inhibitory action of an imidazole-dioxolane compound on heme oxygenase. *Biochemistry,* **2007**, *46*(7), 1860-1867.
http://dx.doi.org/10.1021/bi062264p PMID: 17253780

[103] Rahman, M.N.; Vukomanovic, D.; Vlahakis, J.Z.; Szarek, W.A.; Nakatsu, K.; Jia, Z. Structural insights into human heme oxygenase-1 inhibition by potent and selective azole-based compounds. *J. R. Soc. Interface,* **2013**, *10*(78), 20120697.
http://dx.doi.org/10.1098/rsif.2012.0697 PMID: 23097500

[104] Rahman, M.N.; Vlahakis, J.Z.; Vukomanovic, D.; Lee, W.; Szarek, W.A.; Nakatsu, K.; Jia, Z. A novel, "double-clamp" binding mode for human heme oxygenase-1 inhibition. *PLoS One,* **2012**, *7*(1), e29514.
http://dx.doi.org/10.1371/journal.pone.0029514 PMID: 22276118

[105] Rahman, M.N.; Vlahakis, J.Z.; Roman, G.; Vukomanovic, D.; Szarek, W.A.; Nakatsu, K.; Jia, Z. Structural characterization of human heme oxygenase-1 in complex with azole-based inhibitors. *J. Inorg. Biochem.,* **2010**, *104*(3), 324-330.
http://dx.doi.org/10.1016/j.jinorgbio.2009.10.011 PMID: 19917515

[106] Rahman, M.N.; Vlahakis, J.Z.; Vukomanovic, D.; Szarek, W.A.; Nakatsu, K.; Jia, Z. X-ray crystal structure of human heme oxygenase-1 with (2R,4S)-2-[2-(4-chlorophenyl) ethyl]-2-[(1H-imidazol-1-yl)methyl]-4[((5-trifluoromethyl-pyridin-2-yl)thio)methyl]-1,3-dioxolane: a novel, inducible binding mode. *J. Med. Chem.,* **2009**, *52*(15), 4946-4950.
http://dx.doi.org/10.1021/jm900434f PMID: 19601578

[107] Rahman, M.N.; Vlahakis, J.Z.; Szarek, W.A.; Nakatsu, K.; Jia, Z. X-ray crystal structure of human heme oxygenase-1 in complex with 1-(adamantan-1-yl)-2-(1H-imidazol-1-yl)ethanone: a common binding mode for imidazole-based heme oxygenase-1 inhibitors. *J. Med. Chem.,* **2008**, *51*(19), 5943-5952.
http://dx.doi.org/10.1021/jm800505m PMID: 18798608

[108] Matsui, T.; Iwasaki, M.; Sugiyama, R.; Unno, M.; Ikeda-Saito, M. Dioxygen activation for the self-degradation of heme: reaction mechanism and regulation of heme oxygenase. *Inorg. Chem.,* **2010**, *49*(8), 3602-3609.
http://dx.doi.org/10.1021/ic901869t PMID: 20380462

[109] Noguchi, M.; Yoshida, T.; Kikuchi, G. Purification and properties of biliverdin reductases from pig spleen and rat liver. *J. Biochem.,* **1979**, *86*(4), 833-848.
http://dx.doi.org/10.1093/oxfordjournals.jbchem.a132615 PMID: 40968

[110] Kutty, R.K.; Maines, M.D. Purification and characterization of biliverdin reductase from rat liver. *J. Biol. Chem.,* **1981**, *256*(8), 3956-3962.
PMID: 7217067

[111] Maines, M.D.; Trakshel, G.M. Purification and characterization of human biliverdin reductase. *Arch. Biochem. Biophys.,* **1993**, *300*(1), 320-326.
http://dx.doi.org/10.1006/abbi.1993.1044 PMID: 8424666

[112] Yamaguchi, T.; Yamaguchi, N.; Nakajima, H.; Komoda, Y.; Ishikawa, M. Separation and identification of the isomers of biliverdin-IX and biliverdin-IX dimethyl ester by means of high performance liquid chromatography. *Proc. Jpn. Acad., Ser. B, Phys. Biol. Sci.,* **1978**, *55*, 84-88.
http://dx.doi.org/10.2183/pjab.55.84

[113] Ahmed, F.H.; Mohamed, A.E.; Carr, P.D.; Lee, B.M.; Condic-Jurkic, K.; O'Mara, M.L.; Jackson, C.J. Rv2074 is a novel F420 H2 -dependent biliverdin reductase in *Mycobacterium tuberculosis*. *Protein Sci.,* **2016**, *25*(9), 1692-1709.
http://dx.doi.org/10.1002/pro.2975 PMID: 27364382

[114] Franklin, E.; Browne, S.; Hayes, J.; Boland, C.; Dunne, A.; Elliot, G.; Mantle, T.J. Activation of biliverdin-IXalpha reductase by inorganic phosphate and related anions. *Biochem. J.,* **2007**, *405*(1), 61-67. http://dx.doi.org/10.1042/BJ20061651 PMID: 17402939

[115] Sun, D.; Sato, M.; Yoshida, T.; Shimizu, H.; Miyatake, H.; Adachi, S.; Shiro, Y.; Kikuchi, A. Crystallization and preliminary X-ray diffraction analysis of a rat biliverdin reductase. *Acta Crystallogr. D Biol. Crystallogr.,* **2000**, *56*(Pt 9), 1180-1182. http://dx.doi.org/10.1107/S0907444900008520 PMID: 10957639

[116] Watanabe, A.; Hirata, K.; Hagiwara, Y.; Yutani, Y.; Sugishima, M.; Yamamoto, M.; Fukuyama, K.; Wada, K. Expression, purification and preliminary X-ray crystallographic analysis of cyanobacterial biliverdin reductase. *Acta Crystallogr. Sect. F Struct. Biol. Cryst. Commun.,* **2011**, *67*(Pt 3), 313-317. http://dx.doi.org/10.1107/S1744309110053431 PMID: 21393834

[117] Takao, H.; Hirabayashi, K.; Nishigaya, Y.; Kouriki, H.; Nakaniwa, T.; Hagiwara, Y.; Harada, J.; Sato, H.; Yamazaki, T.; Sakakibara, Y.; Suiko, M.; Asada, Y.; Takahashi, Y.; Yamamoto, K.; Fukuyama, K.; Sugishima, M.; Wada, K. A substrate-bound structure of cyanobacterial biliverdin reductase identifies stacked substrates as critical for activity. *Nat. Commun.,* **2017**, *8*, 14397. http://dx.doi.org/10.1038/ncomms14397 PMID: 28169272

[118] Ahmad, Z.; Salim, M.; Maines, M.D. Human biliverdin reductase is a leucine zipper-like DNA-binding protein and functions in transcriptional activation of heme oxygenase-1 by oxidative stress. *J. Biol. Chem.,* **2002**, *277*(11), 9226-9232. http://dx.doi.org/10.1074/jbc.M108239200 PMID: 11773068

[119] Salim, M.; Brown-Kipphut, B.A.; Maines, M.D. Human biliverdin reductase is autophosphorylated, and phosphorylation is required for bilirubin formation. *J. Biol. Chem.,* **2001**, *276*(14), 10929-10934. http://dx.doi.org/10.1074/jbc.M010753200 PMID: 11278740

[120] Maines, M.D.; Ewing, J.F.; Huang, T.J.; Panahian, N. Nuclear localization of biliverdin reductase in the rat kidney: response to nephrotoxins that induce heme oxygenase-1. *J. Pharmacol. Exp. Ther.,* **2001**, *296*(3), 1091-1097. PMID: 11181945